



Calibration of a distributed hydrology and land surface model using energy flux measurements

Larsen, Morten Andreas Dahl; Refsgaard, Jens Christian; Jensen, Karsten H.; Butts, Michael B.; Stisen, Simon; Mollerup, Mikkel

Published in:
Agricultural and Forest Meteorology

Link to article, DOI:
[10.1016/j.agrformet.2015.11.012](https://doi.org/10.1016/j.agrformet.2015.11.012)

Publication date:
2016

Document Version
Peer reviewed version

[Link back to DTU Orbit](#)

Citation (APA):
Larsen, M. A. D., Refsgaard, J. C., Jensen, K. H., Butts, M. B., Stisen, S., & Mollerup, M. (2016). Calibration of a distributed hydrology and land surface model using energy flux measurements. *Agricultural and Forest Meteorology*, 217, 74–88. <https://doi.org/10.1016/j.agrformet.2015.11.012>

General rights

Copyright and moral rights for the publications made accessible in the public portal are retained by the authors and/or other copyright owners and it is a condition of accessing publications that users recognise and abide by the legal requirements associated with these rights.

- Users may download and print one copy of any publication from the public portal for the purpose of private study or research.
- You may not further distribute the material or use it for any profit-making activity or commercial gain
- You may freely distribute the URL identifying the publication in the public portal

If you believe that this document breaches copyright please contact us providing details, and we will remove access to the work immediately and investigate your claim.

Manuscript Number: AGRFORMET-D-15-00325R1

Title: Calibration of a distributed hydrology and land surface model
using energy flux measurements

Article Type: Research Paper

Section/Category: Energy Budget

Keywords: hydrology/land surface modelling; calibration; water and energy
fluxes; evapotranspiration; energy closure imbalance

Corresponding Author: Dr. Morten Andreas Dahl Larsen, Ph.D.

Corresponding Author's Institution: Technical University of Denmark

First Author: Morten Andreas Dahl Larsen, Ph.D.

Order of Authors: Morten Andreas Dahl Larsen, Ph.D.; Jens C Refsgaard,
Dr. Scient; Karsten H Jensen, Ph.D.; Michael B Butts, Ph.D.; Simon
Stisen, Ph.D.; Mikkel Mollerup, Ph.D.

Abstract: In this study we develop and test a calibration approach on a spatially distributed groundwater-surface water catchment model (MIKE SHE) coupled to a land surface model component with particular focus on the water and energy fluxes. The model is calibrated against time series of eddy flux measurements from three sites of different land surface type (agriculture, forest and meadow) and river discharge data from the 2500 km² Skjern River catchment in Denmark. The approach includes initial calibrations of three one-dimensional models representing the three land surface types using the flux measurements for calibration. This step provides initial values for the subsequent modelling and calibration at catchment scale. To test the validity of the approach, two additional catchment scale distributed simulations were performed with no calibration and only calibration of the one-dimensional models, respectively. In addition, a subsequent validation period was simulated. A mean energy closure imbalance of 20% was seen for the three sites. For the distributed simulations, the energy imbalance was accounted for by two energy balance closure hypotheses ascribing the error to either energy fluxes or net radiation. In general, the distributed calibration approach improved model results substantially compared to using default values (no calibration) or calibration of the one-dimensional models only. For the distributed model simulations, the assumption regarding the energy balance closure had a substantial impact on the parameter sensitivities and on the simulated discharge and energy balance. During calibration, the simulation with corrected energy fluxes showed better performance on discharge than the simulation with corrected net radiation whereas the reverse was true for the validation period. Regarding energy fluxes, the simulation with corrected net radiation was superior in both the calibration and validation period.

19/5-2015

Dear Editor

With great pleasure we hereby submit our research paper “*Calibration of a distributed hydrology and land surface model using energy flux measurements*” for consideration in the Journal of Agricultural and Forest Meteorology.

Traditionally, distributed hydrology models often rely on potential evapotranspiration to estimate actual evapotranspiration rather than solving the energy equation. SVATs and LSMs on the other hand do solve the energy equation and are often calibrated in 1D or use remote sensing data in distributed setups.

With the present paper we present a novel approach to calibrating a combined spatially distributed hydrology-land surface model using energy flux tower observations in combination with discharge reaching good results.

The present paper is not a resubmission and has no concurrent submissions to other journals.

Sincerely, Morten A D Larsen, corresponding author, madla@dtu.dk/+4525119895

Ms. Ref. No.: AGRFORMET-D-15-00325

Title: Calibration of a distributed hydrology and land surface model using energy flux measurements
Agricultural and Forest Meteorology

I have now completed the review of the above manuscript. I apologize for the unusually long review time. We invited 14 different reviewers to assess your work. I have decided to make a decision based on one review and my own assessment of your manuscript.

In my opinion, the manuscript is extremely well written and addresses an important topic. I appreciate the objective and rigorous calibration approach and the testing of the models at the eddy covariance sites and catchment scales. This manuscript was a pleasure to read. I have a few minor comments/questions:

Dear editor/co-editor and reviewers

Thank you for considering our manuscript, the overall positive critique, the large effort in finding reviewers and the reviews itself which address important points even in the light of the suggested “minor review”. Below you find a comment by comment reply to the points raised by the two reviewers.

Best regards,

Morten A. D. Larsen

1. I wondered how much of the ag land is tile drained and how this might influence the model performance compared to the non ag lands?

Being a part of the DK-model nationwide MIKE SHE setup a global (100% coverage) drainage is used since the dense network of smaller streams and ditches cannot be resolved by the 500 m resolution. The differences between land surface types should therefore be minimal. The drainage is described in:

Henriksen, H.J., Trolborg, L., Højberg, A.L., Refsgaard, J.C., 2008. Assessment of exploitable groundwater resources of Denmark by use of ensemble resource indicators and a numerical groundwater–surface water model. *Journal of Hydrology* 348, 224–240. doi:10.1016/j.jhydrol.2007.09.056

At the scale in question the setup is capable of reproducing observed physical variables such as discharge, groundwater heads and soil moisture due to rigorous calibration and refinement during the last 12-15 years. We do not have information on the exact share of drained land over the agricultural areas within the catchment, but refer to technical papers on the performance of specific output variables:

Henriksen, H.J., Trolborg, L., Nyegaard, P., Sonnenborg, T.O., Refsgaard, J.C., Madsen, B., 2003. Methodology for construction, calibration and validation of a national hydrological model for Denmark. *Journal of Hydrology* 280, 52–71. doi:10.1016/S0022-1694(03)00186-0

2. Line 193. you mention simulated irrigation, but it is not clear how much water this adds to the system or how you determined the simulated amount. Further, how much uncertainty does this add to your analysis?

The irrigation is calculated in the MIKE SHE model code on the basis of knowledge on well locations, filter depths, known annual abstraction, a demand area and agricultural land around each well by a demand function and a simulated water deficit in the root zone as described in:

Stisen, S., Sonnenborg, T.O., Højberg, A.L., Trolborg, L., Refsgaard, J.C., 2011b. Evaluation of Climate 748 Input Biases and Water Balance Issues Using a Coupled Surface–Subsurface Model. *Vadose Zone J.* 10, 749–757. doi:10.2136/vzj2010.0001

To be able to add irrigation to the precipitation file, these simulations have however been performed prior to the simulations were results are extracted for this manuscript. We agree that this is currently not clear in the manuscript and have revised accordingly. Good suggestion.

3. You do a nice job assessing the impact of lack of energy balance closure and showing the sensitivity to such assumptions. I recommend you include in your discussion some of Alan Barr's work.

Energy balance closure at the BERMS flux towers in relation to the water balance of the White Gull Creek watershed 1999-2009

By: Barr, A. G.; van der Kamp, G.; Black, T. A.; et al.

AGRICULTURAL AND FOREST METEOROLOGY Volume: 153 Special Issue: SI Pages: 3-13

Published: FEB 15 2012

Thank you very much. We have been aware that some would think the paper is on the heavy side with regards to the number of references which is partly caused by the literature study on parameter values. Other than the included studies on parameter values, the number of studies on energy balance closure is of course vast and the number of references to include among these is a subjective matter. We are glad to be made aware of this study and definitely agree that it should be included due to the catchment scale, energy balance considerations, the long evaluation period and streamflow evaluation. This is done.

It would be helpful to me if you could return the reviews annotated, in a different colour or font, to indicate how you have responded to each of the comments.

I am not sure if you mean in the response letter or in a manuscript version but I do both to make sure: In the present document I answer each comment separately and point out where I have applied the corrections and I also attach a manuscript version with corrections highlighted.

Reviewers' comments:

Reviewer #1: Summary of Paper:

The objective of this work is to develop a method for parameter calibration of a spatially distributed hydrologic model using both energy fluxes and catchment runoff. The study used the MIKE SHE hydrologic model and the SWET land surface model. The authors conducted a parameter sensitivity test (Monte-Carlo) and presented four stepwise calibration schemes.

Main impression:

The approach used in this paper was novel, complex, and adds great understanding to the parameterization of distributed hydrologic models. Their results do show an overall improvement in the simulated energy balance post-calibration. I would suggest very minor edits/additions prior to publication.

As also stated above – we would like to thank for the effort in reviewing and the positive judgement of the paper.

Specific Comments and Suggestions:

1. L22: "...the three land surface types and using the flux measurements for calibration."
I am not sure what is suggested here? The above text is exactly equal to the manuscript and can therefore not be seen as a suggestion for a change. After reading the sentence again I can see that the "and" could be removed which could have been the intent of the suggestion. This is done.
2. L29: Are you referring to the calibration approach of the distributed systems?
Yes – this is specified.
3. L46: Explain acronyms before use.
We agree fully but these are model names which was not clear. This is therefore clarified.
4. L94-95: Sentence error.
That sentence was indeed uneasy. It was corrected in relation to including a reference as suggested by the editor:
(Barr, A.G., van der Kamp, G., Black, T.A., McCaughey, J.H., Nesic, Z., 2012. Energy balance closure at the BERMS flux towers in relation to the water balance of the White Gull Creek watershed 1999–2009. Agric. Forest Meteorol. 153, 3–13. doi:10.1016/j.agrformet.2011.05.017).
5. L130: Referring the outlier and replacement data in Line 130 - Can the authors expand on how much data was considered an outlier and removed in the results section? Or was any data removed from the calibration/validation periods? This is important since both periods are only 1 year.
We agree that this could potentially infer with the quality of the calibration results and could be addressed in quantitative terms in addition to using the reference (Ringgard et al. 2012). For the calibration period the LE outliers made up 0.16%, 0.74%, 0.13% of the data material for Agriculture, forest and meadow respectively and for H the corresponding numbers were 0.05%, 0.8% and 0.15%. In essence a relative small portion of the data. We have added the outlier-replaced percentage between LE and H to the text (weighted average between stations).

6. Section 4.2 - By this section I already forgot about what HYP1, 2, 3, 4 represented as far as the calibration scheme. Adding a short sentence reminding the reader about the calibration approaches would be helpful.

Good suggestion. This is added.

7. Figure 4. Agriculture - Root shape parameter - I'm a little baffled as to how the input scenarios affect the parameter sensitivity so much as to designate the parameter highly sensitive for HYP1 and HYP4 (100% sensitivity), and moderately sensitive (<40%) for the other two scenarios. This is the same site, the inputs should not be so different.

We agree that from an immediate understanding the difference should not be in this range. More conditions could however attribute to this:

- The sensitivities are relative and therefore the change in relative root shape (A_root) sensitivity can be caused by changes in sensitivities for other parameters – in this case Rst_min.
- The processes are highly non-linear causing this shift when using either corrected (HYP1 and HYP4) or uncorrected fluxes (HYP2 and HYP3).
- The root shape parameter controls the distribution of root water uptake from either the upper or lower part of the root zone. Thus, it appears that this parameter, as opposed to root depth, is the most effective when adjusting for a simulated reproduction of actual evapotranspiration.

8. Figure 8. Add x and y labels

We have only written labels once, since they are equal for all three figures. We have however changed the layout slightly to more clearly reflect this.

For further assistance, please visit our customer support site at

<http://help.elsevier.com/app/answers/list/p/7923>. Here you can search for solutions on a range of topics. You will also find our 24/7 support contact details should you need any further assistance from one of our customer support representatives.

Highlights

- A new hydrology model calibration approach solving the energy equation is proposed.
- Initial 1D calibration is performed on three representative flux tower sites.
- LE+H+G were 20% below Rn requiring two hypotheses on the erroneous component.
- The approach was skilful – validated against runs with fewer calibration steps.
- The hypothesis ascribing Rn error was superior over the LE+H+G error hypothesis.

Calibration of a distributed hydrology and land surface model using energy flux measurements

Morten A. D. Larsen^{1*}, Jens C. Refsgaard², Karsten H. Jensen³, Michael B. Butts⁴, Simon Stisen² and Mikkell Møllerup⁵.

1 - Technical University of Denmark, Department of Management Engineering, Frederiksborgvej 399, 4000 Roskilde, Denmark

2 - Geological Survey of Denmark and Greenland, Øster Voldgade 10, 1350 Copenhagen, Denmark.

3 - University of Copenhagen, Department of Geosciences and Natural Resource Management, Øster Voldgade 10, 1350 Copenhagen, Denmark.

4 - DHI, Agern Alle 5, DK 2970, Hørsholm, Denmark

5 - The Danish Road Directorate, Guldalderen 12, 2640 Hedehusene.

* - Corresponding author: madla@dtu.dk/004525119895

Keywords: hydrology/land surface modelling; calibration; water and energy fluxes; evapotranspiration; energy closure imbalance

1 Abstract

In this study we develop and test a calibration approach on a spatially distributed groundwater-surface water catchment model (MIKE SHE) coupled to a land surface model component with particular focus on the water and energy fluxes. The model is calibrated against time series of eddy flux measurements from three sites of different land surface type (agriculture, forest and meadow) and river discharge data from the 2500 km² Skjern River catchment in Denmark. The approach includes initial calibrations of three one-dimensional models representing the three land surface types using the flux measurements for calibration. This step provides initial

values for the subsequent modelling and calibration at catchment scale. To test the validity of the approach, two additional catchment scale distributed simulations were performed with no calibration and only calibration of the one-dimensional models, respectively. In addition, a subsequent validation period was simulated. A mean energy closure imbalance of 20% was seen for the three sites. For the distributed simulations, the energy imbalance was accounted for by two energy balance closure hypotheses ascribing the error to either energy fluxes or net radiation. In general, the distributed calibration approach improved model results substantially compared to using default values (no calibration) or calibration of the one-dimensional models only. For the distributed model simulations, the assumption regarding the energy balance closure had a substantial impact on the parameter sensitivities and on the simulated discharge and energy balance. During calibration, the simulation with corrected energy fluxes showed better performance on discharge than the simulation with corrected net radiation whereas the reverse was true for the validation period. Regarding energy fluxes, the simulation with corrected net radiation was superior in both the calibration and validation period.

40

41 **2 Introduction**

Water and energy fluxes between land surface and atmosphere are important components of atmospheric and hydrological processes. These fluxes can be quantified by the use of land surface models (LSM) or soil-vegetation-atmosphere-transfer models (SVAT). The calculation of e.g. evapotranspiration in SVATs and LSMs is based on solving the energy and radiation equations often on a sub-daily basis and they therefore differ from the less physically stringent schemes often used in many traditional hydrological models which are based on potential evapotranspiration. LSMs, originating from atmospheric sciences, include spatially distributed, often large scale descriptions of land surface processes. Examples include the Noah model (Rosero et al. 2010) and the CLM model

50 (Lawrence et al. 2011). LSMs are typically coupled with or forced by atmospheric models and have
51 recently been included in fully coupled climate-hydrology models (Maxwell et al. 2011, Shrestha et
52 al. 2014). SVATs, originating from soil and hydrological sciences, are one-dimensional descriptions
53 typically used for small-scale descriptions linked with soil water flow models (Mauser and
54 Schädlich 1998, Ridler et al. 2012). When included in spatially distributed hydrological models they
55 possess the potential for providing improved evapotranspiration descriptions and enable
56 hydrological catchment models to better utilise remote sensing data to force and constrain
57 hydrological models (Stisen et al. 2011a). SVATs have also recently been included in fully coupled
58 climate-hydrology models (Butts et al. 2014, Larsen et al. 2014). LSMs and SVATs linked to
59 spatially distributed hydrological models are basically similar, and hence we shall in the following
60 refer to both of them as SVAT models.

61 Assessment of parameter values is critical for the use of SVAT models and an essential
62 challenge is related the vast number of parameters often seen in this type of models. Franks et al.
63 (1997, 1999), Beven and Franks (1999) and Gupta et al. (1999) all highlight the high uncertainty in
64 the predictive capabilities of multi-parameter SVATs due to equifinality. Yet; Franks et al. (1997,
65 1999) still show good results in terms of reproducing point site flux measurements from the FIFE
66 area in Kansas, USA, and in the Amazon area in Brazil. The added value of a multi-criteria
67 approach as opposed to a single criterion method is confirmed by Gupta et al. (1999) and Demarty
68 et al. (2004). Pollacco et al. (2013) apply an objective function weighing algorithm based on the
69 uncertainties related to remote sensing based surface soil moisture and evapotranspiration
70 calibration variables. Currently no explicit guidelines have been developed on calibrating complex
71 and distributed SVAT and hydrology models.

72 Parameter estimation for hydrological models is traditionally performed by use of
73 calibration where parameter values are modified to obtain best possible fit between model

74 simulations and observed target data. While calibration was previously often performed manually
75 by a trial-and-error approach, parameter optimisation by inverse modelling is now the method of
76 choice (Gupta et al. 1998, Madsen 2003, Moore and Doherty 2005). An example is the study by Sun
77 et al. (2013) where inverse calibration based on Monte Carlo-Bayesian techniques was used for
78 calibrating a model both against energy fluxes at point scale and runoff at catchment scale (4.9
79 km²). In Ingwersen et al. (2011) inverse calibration was used to simulate the water and energy
80 budget for a winter wheat stand at plot scale. Similarly Ridler et al. (2012) utilized inverse
81 techniques for calibrating the combined MIKE SHE/SWET model to simulate energy fluxes at point
82 scale in Mali.

83 A particular problem related to calibration of SVAT models is that observations of water and
84 energy fluxes are usually not available from operational monitoring networks but only from a few
85 research stations and often for short periods (Wilson et al. 2002, Franssen et al. 2010, Leuning et al.
86 2012). In addition, energy flux data are known to often have problems with energy balance closure
87 which severely hampers parameter optimisation by inverse modelling, as a SVAT model per
88 definition assumes a closed energy balance (Twine et al. 2000, Choi et al. 2009) and a failure to
89 meet this demand can result in significant biases in long term climate model simulations
90 (Grimmond et al. 2010). Also, the lack of measured energy balance closure will yield an erroneous
91 parameterization when the fluxes are used for the calibration of a hydrological model. Therefore
92 certain assumptions need to be made to account for the lack of closure. To accommodate this,
93 Beven (2006) suggested creating artificial hypotheses to provide closure.

94 Catchment water balances are linked to energy balances, because the latent
95 energy/evapotranspiration appears as a key element in both balances. The observed catchment
96 runoff and the catchment water balance assessed by hydrological models hence include important
97 information also on the energy balance. On a catchment scale (603 km²) Barr et al. (2012) used

distributed flux tower measurements of evapotranspiration against measured precipitation and discharge for a residual analysis on water balance closure concluding a 15% lack of energy flux closure compared to the measured net energy. For catchment scale (205 km²) model calibration, Li et al. (2011) used the CLM4 model, modified to include a runoff scheme, to evaluate both runoff and energy fluxes. Similarly, operating on a regional to continental scale Maurer et al. (2002) simulated energy flux components while the model was manually calibrated only against runoff.

The objectives of the present study is to develop and test a methodology for calibrating and assessing parameters of a SVAT model linked to a spatially distributed hydrological model by using observations of both energy fluxes and catchment runoff. A comprehensive literature study was carried out to obtain feasible initial values and range of variation for parameters for the considered land surface types. The impact of energy imbalance is of particular emphasis and we analyse to which extent inclusion of discharge observations in the calibration process will improve the model performance and robustness.

111

112 **3 Methodology**

113 **3.1 Study area and data**

The Skjern catchment (2500 km²) is located in the western part of the Jutland peninsula, Figure 1. The catchment is dominated by sandy soils generated by glacial outwash plains from the last glacial period Weichsel and intersected by older till deposits from the previous glacial period Saalian (Greve et al. 2007). The topography reaches 130 m above sea level in the eastern part of the catchment and the Skjern River flow into Ringkøbing fjord at sea level to the west. The yearly average precipitation for the catchment is 940 mm for the period 2000-2009 based on direct measurements. When corrected for undercatch using standard monthly correction factors (Allerup et al. 1998) the average precipitation amounts to 1130 mm. In the same period the mean annual

122 temperature is 9.3 °C and the mean monthly temperatures range between 2.1 and 17.3 °C. Inside the
123 catchment flux towers are placed at the three predominant surface types; agriculture (61%),
124 meadow/grass (24%) and forest (13%), Figure 1. At all sites measurements of short-, long-wave and
125 net radiation components; latent (LE), sensible (H) and soil heat fluxes (G); soil water content;
126 precipitation; air temperature; wind speed; and water table levels have been carried out since late
127 2008. Measurements of radiation and energy fluxes are based on standard methods. Radiation
128 components are measured using a NR01 Hukseflux radiometer (www.hukseflux.com), LI-COR
129 eddy covariance equipment is used for measuring LE fluxes, Gill sonic anemometers for measuring
130 H fluxes, and Hukseflux plates for measuring G fluxes.

131 The energy flux data used in the study have undergone quality control as part of the
132 processing (Ringgard, 2012) (Step 1.3, Figure 2). Inaccurate observations caused by e.g. low
133 turbulence condition were replaced by data representing similar conditions. Replacement of data
134 was thus for periods with low energy fluxes and therefore this source of uncertainty is expected to
135 be of minor significance. Individual data points clearly outside the expected range at the time of day
136 and season were considered as outliers and removed (equal to 0.2% on average between LE, H and
137 the three stations weighted relative the areal share). For two periods July 21-August 16 and August
138 24-October 28, 2009, no flux measurements were available from the agricultural site and data were
139 replaced from the forest site. As these periods are mostly placed in the spin-up period (see below)
140 the calibration results are not expected to be significantly affected.

141

142 **3.2 Modelling system and setup**

143 This study uses the spatially distributed MIKE SHE hydrological modelling system capable
144 of including all key hydrological processes such as ET, channel flow, overland flow, unsaturated
145 flow, saturated flow as well as irrigation and drainage (Graham and Butts 2005). The land surface

146 model SWET component (Overgaard, 2005) is used in the analysis. SWET is based on the
147 Shuttleworth-Wallace model (Shuttleworth and Wallace 1985). It considers vegetation and energy
148 balance processes in a two-layer system and is extended to include energy fluxes from ponded
149 water and interception storage. Models are constructed for both the three local measurement sites
150 (1D representation) and for the entire catchment (Figure 1).

151 The 1D models simulate energy fluxes and vertical unsaturated flow based on Richards'
152 equation. The SWET model is driven by 30 min climatic observations of precipitation, air
153 temperature, wind speed, net radiation, surface air pressure and relative humidity. Measured water
154 table elevations are specified as lower boundary condition. As opposed to the fully distributed
155 model application overland flow, river flow and groundwater flow are not considered. Relevant to
156 both the 1D and distributed analyses, the SWET land-surface module does not consider snow
157 accumulation and melting. Initial values for root depth and vegetation height applicable for the 1D
158 simulations of the agricultural and meadow sites were based on estimates from model simulations
159 for relevant soil type and management conditions using the vegetation model Daisy (Styczen et al.
160 2004a). Since the footprint of the flux tower at the agricultural site was influenced by several crop
161 types, the vegetation height and root depth were based on average simulations for winter- and
162 spring cereals. The observational data for leaf area index (LAI), another important crop parameter,
163 was inconsistent, and the seasonal variation of this parameter was therefore derived by combining
164 the observed seasonal trends and the simulation results by the Daisy model. The initial values for
165 soil parameters for each site were derived from the HYPRES pedotransfer function (Wösten et al.
166 1999). Specifically, the Van Genuchten parameters α and n (van Genuchten, 1980) as well as
167 saturated hydraulic conductivity, residual- and saturated water content were estimated from soil
168 texture, organic matter and bulk density. The soil texture data were retrieved from grid values from
169 a distributed soil map of 250 m resolution in the A horizon (0-30 cm) and 500 m resolution in B and

C horizons (30-80 cm and below 80 cm) (Styczen et al. 2004b, Greve et al. 2007, Iversen et al. 2011). For the sensitivity and optimization analyses the soil parameter bounds were defined by calculating the 90% confidence intervals of variation ranges from Meyer et al. (1997) for soils of similar texture as for the three field sites. These soil types include sand, loamy sand and sandy loam for the agriculture and forest site roughly corresponding to JB1 soil (coarse sand) in the Danish soil classification system (Greve et al. 2007, www.djfgeodata.dk). Due to the lack of agreement on soil type at the meadow site between site specific soil retention data and available soil maps the 90% confidence intervals for the meadow site is based on a wider range of soil types from loamy sand to clay loam (Meyer et al. 1997). The discrepancy of the data is most likely due to highly heterogeneous soils caused by shifting alluvial deposits from the nearby Skjern River. In the parameterization the seasonal patterns of vegetation characteristics as induced by both climate and management practice were kept constant whereas the respective amplitudes were calibrated by a single factor for each parameter. The annual sequence of these ratios was found by balancing model simulations by Daisy, relevant literature values (Table 1) and occasional on-site measurements of LAI and vegetation height. Similarly, the relation between the parameter values in the three vertical soil type horizons were kept constant implying that the individual parameters for the A, B and C horizon were shifted by the same factor for each grid cell. By introducing factors between parameters in space and time the number of parameters to be optimized is reduced.

The MIKE SHE model for catchment scale is based on the Danish national water resources model (DK-model) (Stisen et al. 2012, Højberg et al. 2013). As opposed to the DK-model the present model includes the SWET land-surface model and the parameterization of this model is partly based on the work by Stisen et al. (2011a). The DK model has a 500 m resolution and includes a detailed river network. A maximum time step of 1 hour is used for overland, unsaturated and saturated flow. The MIKE 11 open channel river model component utilizes 3616 cross sections

194 in 100 river branches and uses a 30 min time step. For precipitation exceeding 2 mm per time step
195 an automatic reduction in time step takes place. The input for the catchment scale SWET model is
196 hourly values of the same climatic variables as for the 1D models. These values are obtained by thin
197 plate spline interpolation of climate station data (Stisen et al. 2011a) to a resulting grid in 2 km
198 resolution for all variables except precipitation used in 500 m resolution. Precipitation input is
199 based on interpolation of daily rain gauge data using kriging and dynamically corrected for
200 undercatch. Hereafter, simulated irrigation is added to the precipitation input file. The simulated
201 irrigation is calculated from the root zone deficit and a demand function based on well locations,
202 filter depths, annual abstractions and demand area information (Stisen et al. 2011b). The
203 agricultural crop distribution was developed from statistical data, where the various crops were
204 grouped in four classes with different growth characteristics: spring sown cereals, winter sown
205 cereals, grass/clover and maize. The crop classes were distributed without georeferencing due to
206 lack of data. Forest vegetation parameters were based on relevant literature and observations. A
207 total of 36 parameters were analysed in the sensitivity analysis. As the calibration is targeted
208 towards the energy fluxes no sensitivity and calibration analyses are performed on the saturated
209 zone parameterization which is already well calibrated as a part of the DK-model (Stisen et al.
210 2012, Højberg et al. 2013).

211 To generate proper initial conditions for soil moisture in the 1D simulations a spin-up period
212 of 5-10 months prior to the calibration period was used. The spin-up periods were decided by data
213 availability as measurements started in April 2009 for the agriculture and meadow sites and
214 December 2008 for the forest site. The distributed model involves a considerable increase in
215 computation time compared to the 1D setups and a spin-up period of 3 months was therefore used.
216 Groundwater quasi steady-state was reached by looping simulations in 3-year runs each time using

217 the resulting groundwater heads as initial conditions for the subsequent simulation. Three loops
218 were required to reach quasi steady-state.

219

220 **3.3 Calibration approach**

221 We propose a calibration and validation approach involving three steps as illustrated in
222 Figure 2: (1) calibration of 1D models representing the flux measurement sites, (2) use of parameter
223 values from step 1 as initial values in the calibration of the distributed catchment model, and (3)
224 validation of the distributed parameterization on independent data. Additionally we test the
225 calibration results by comparing to model results based on 1D calibration only and with no
226 calibration respectively.

227 Both the 1D and the distributed simulations were calibrated using inverse modelling
228 adopting initial and range of parameter values from literature, observations, databases and
229 simulation results from the model code Daisy (Hansen et al. 1990, 1991) as described above and as
230 listed in Table 1 and 2. The initial input parameter values as well as their ranges were specified
231 according to relevance: If available, either observations or Daisy model simulations based on site
232 specific conditions were used. When using literature values conditions similar to the sites in terms
233 of vegetation species, climate and soil type were used. The calibration period covers a one year
234 period from October 1, 2009 to September 30, 2010 while the validation period is from May 1,
235 2011 to April 30, 2012.

236 The sensitivity and auto-calibration analyses were performed using the AUTOCAL software
237 included in the MIKE SHE package (Madsen 2003). At the point scale three components were
238 included in the objective function: latent heat flux LE, sensible heat flux H, and averaged soil water
239 content based on measurements at three depths (2.5, 22.5 and 52.5 cm below the surface). The
240 objective function was built from the root mean square errors (RMSE) between observations and

simulations. The RMSEs for the three individual components were normalized, weighted equally and summed to arrive at an aggregated objective function. The normalization was carried out using the common distance scale which has proven to be robust in accounting for differences in magnitude of each component of the objective function (Madsen 2003, Butts et al. 2004, Mertens et al. 2004).

At catchment scale the optimization was performed against two overall components of equal weight: (1) Discharge observations at three discharge stations aggregated with equal weight (Figure 1) and (2) latent and sensible energy fluxes at the three sites weighted according to the relative areal share of each land surface type (agriculture 62%, forest 13% and grass/meadow 25%).

The sensitivity analysis (Step 1.2 and 2.2 in Figure 2) for both point and catchment scales were based on the AUTOCAL local sensitivity analysis procedure accounting for parameter sensitivities at the location in parameter space defined by the initial parameter values. Since the sensitivity analysis was local and therefore unable to account for numerous combinations in the parameter space, the sensitivity analyses were repeated using randomly sampled parameter sets within the parameter bounds. The sensitivity analysis was based on a backward difference approximation method around the parameter value using a 2% perturbation fraction. Also, covariance matrices were calculated to test for parameter correlation.

For both scales the ten most sensitive parameters were identified and subsequently used in the auto-calibration process similar to Blasone et al. (2007). Only parameters with relative sensitivity coefficients above 1%, in relation to the most sensitive parameter, were included in the optimization (Hill 1998). For the low sensitivity parameters that were not included in the auto-calibration of the catchment model their values were derived from the point scale calibrations. The remaining distributed parameters were based on relevant literature (Table 2).

264 The point scale parameter optimization was based on the global Shuffled Complex
265 Evolution method (Duan et al. 1993) which has proven to be robust for comprehensive parameter
266 estimation problems (Butts et al. 2004, Mertens et al. 2005, Blasone et al. 2007). A maximum time
267 step of 6 minutes was used for the 1D models, which for the calibration period corresponded to a
268 computation time of around 2-3 minutes per model run. The model convergence criteria were
269 defined as max. 1% change in objective function after three iterations loops and this criterion was
270 usually met after 200-250 runs. For obtaining a more efficient optimization of the catchment scale
271 model, parallel model runs were carried out using the global Population Simplex Evolution
272 optimization method (DHI 2010). The convergence criterion was typically reached after 250-400
273 runs.

274 To assess the accuracy of the parameterization and modelling approach as such, an
275 independent validation analysis was performed subsequent to the auto-calibration simulations. The
276 validation was performed for a one-year period and assessed on discharge, LE and H as for the
277 calibration analysis (Step 3.1, Figure 2).

278

279 **3.4 Handling of Energy Balance Flux problems**

280 Energy balance closure requires that the net radiation (difference between incoming and
281 outgoing long- and short-wave radiation) equals the sum of latent heat (LE), sensible heat (H), and
282 soil heat (G) fluxes. All terms are highly sensitive to the surface characteristics and furthermore
283 they are subject to different diurnal and seasonal variations. The albedo of bare soil is dependent on
284 texture and moisture content while the albedo for vegetation generally decreases with vegetation
285 height and stand complexity. Changes in albedo will affect the amount of available energy, and soil
286 moisture influences how this energy is distributed between LE and H heat fluxes. Independent
287 measurements of the components of the energy balance equation rarely provide closure, which has

288 been documented in numerous studies (Wilson et al. 2002, Franssen et al. 2010, Leuning et al.
289 2012).

290 The impact of the energy balance closure problem on the calibration results was addressed
291 by creating four hypotheses each based on different assumptions regarding measurement errors
292 (Step 1.4 and 2.4, Figure 2). All four hypotheses were used for the 1D runs whereas only the first
293 two were used in the distributed runs to reduce computation time.

- 294 • HYP1: The measured energy fluxes (LE, H and G) are scaled with a single factor (increase)
295 such that the Bowen-ratio is maintained and the sum of the energy fluxes equals measured
296 net radiation over the one-year calibration period;
- 297 • HYP2: The measured energy fluxes are maintained whereas the net radiation is scaled with a
298 factor (reduction) to match the sum of measured energy fluxes over the one-year calibration
299 period;
- 300 • HYP3: The measured energy fluxes are unaltered whereas the sum of these is used as net
301 radiation on a daily basis;
- 302 • HYP4: The measured energy fluxes (LE, H and G) are scaled with a single factor (increase)
303 such that the Bowen-ratio is maintained and the sum of the energy fluxes equals measured
304 net radiation on a daily basis;

305 For the first two scenarios the entire dataset is multiplied by a single scaling factor to
306 provide energy closure for the one year calibration period. Closure on a daily basis may not be met,
307 which is the case for the last two scenarios. Of the investigated scenarios more energy is available
308 in HYP1 and HYP4 based on the measured net radiation (yearly mean values of 55 w/m^2 , 68 w/m^2
309 and 55 w/m^2 for agriculture, forest and meadow respectively) whereas HYP2 and HYP3 are based
310 on reduced values (yearly mean values of 39 w/m^2 , 48 w/m^2 and 42 w/m^2 for the same sites).

311 Only the HYP1 and HYP2 hypotheses were used for the distributed simulations since they
312 both utilize measured net radiation, scaled and unscaled, and hereby the daily temporal pattern is
313 likely to be more representative than if based on the sum of the three fluxes. In contrast to the point
314 scale where net radiation measurements were available, global radiation was used in the catchment
315 scale analysis. To fulfil the same assumptions on energy balance closure as used at point scale the
316 albedo was adjusted to obtain energy balance closure over the entire one year calibration period.
317 This was done based on the flux measurements for the three general land use types agriculture,
318 forest and meadow. As a result HYP1 is based on measured albedos whereas HYP2 is based on
319 estimated albedos that are higher than measured. All three distributed simulation cases shown in
320 Figure 2 were performed for both HYP1 and HYP2 as well as for the calibration and validation
321 periods for a total of 12 simulations.

322

323 **4 Results**

324 **4.1 Energy balance closure**

325 The measurements used in this study show lack of energy balance closure. The sum of LE,
326 H and G over the one-year calibration period accounted for 71%, 71% and 76% of the measured net
327 radiation at the agricultural, forest and meadow/grass sites respectively (Figure 3). The
328 corresponding measured Bowen-ratios in the same period were 0.20, 0.17 and 0.18 for the three
329 land surface types. Radiation and particularly data for energy fluxes are generally sparse in
330 Denmark. Therefore, in Figure 3, measured net and global radiation as well as the sum of energy
331 fluxes are compared to results from (1) the corresponding grid cell in HIRHAM regional climate
332 model simulations (Larsen et al. 2013) using ERA-Interim reanalysis data as boundary conditions
333 and (2) observation data from the Foulum research station (grass surface) located app. 50 km north
334 of the agriculture and forest sites. HIRHAM simulation data are also used to compare LE and H

335 fluxes since no other flux data were available. The simulations of net radiation by HIRHAM and the
336 observed data from Foulum are much closer to measured LE, H and G flux sum at all sites for both
337 years although perhaps less distinct at the forest site (Figure 3). For global radiation there is a close
338 match between all data series, especially between the three study sites and Foulum. For LE fluxes
339 good agreement is seen between HIRHAM simulations and observations for the forest and meadow
340 sites and less favourable for the agricultural site. For the H fluxes larger discrepancies are seen
341 particularly for the forest site.

342

343 **4.2 Simulation results**

344 The results of the sensitivity analyses for both point and catchment scales are shown in
345 Figure 4. Similar parameter sensitivity results are obtained for the agricultural and forest sites with
346 nine and ten parameters, respectively, having a relative sensitivity coefficient above 10%. The
347 parameter sensitivities for hypotheses HYP2 and HYP3 (with unaltered energy fluxes) show similar
348 patterns with the minimal stomata resistance (R_{st_min}) as the most sensitive parameter. In contrast,
349 for hypotheses HYP1 and HYP4 (with corrected energy fluxes) the root shape factor is the most
350 sensitive parameter. For the meadow site only the three parameters R_{st_min} , leaf area index (LAI)
351 and vegetation height have relative sensitivity coefficients above 10% and the influence of the
352 energy balance hypothesis is limited given the large drop in sensitivity between R_{st_min} and the
353 second most sensitive parameter LAI.

354 At catchment scale saturated hydraulic conductivity (K_{sat}) for the unsaturated zone is the
355 most sensitive parameter for both energy balance hypotheses, whereas the sensitivities of the
356 remaining parameters are smaller and also subject to larger variation between the two hypotheses
357 (Figure 4). The forest energy fluxes were found to be poorly reproduced by the calibrated forest leaf
358 width values which were therefore manually calibrated prior to auto-calibration.

359 The simulated discharge based on the parameter values obtained by the full auto-calibration
360 approach for the two distributed energy balance hypotheses are shown in Figure 5 for both the
361 calibration and validation periods. For both simulations and periods there is a tendency of
362 underestimation of baseflow and mostly pronounced for HYP2. For peak flow the HYP2 hypothesis
363 exhibits more dynamic behaviour with more rapid responses. In summary, the HYP1 simulation
364 shows better discharge performance statistics for the calibration period whereas the opposite pattern
365 is seen for the validation period (Figure 6). Also, the validation confirms a reasonable discharge
366 calibration although the HYP1 results are moderately poorer for two out of three discharge stations.

367 Figure 7 shows simulated LE and H energy fluxes on an hourly basis for a 10 day summer
368 period in the calibration period. The results from the two energy hypothesis runs are compared to
369 their relevant fluxes: HYP1 to scaled and HYP2 to unscaled fluxes, corresponding to the
370 assumptions of the energy balance closure. For both the calibration and validation periods, there is a
371 tendency for better energy flux statistics for HYP2 compared to HYP1 (Figure 6). Overall the
372 agriculture and grass surfaces are better reproduced compared to forest. Especially observations of
373 H in the forest are rather poorly simulated during high global radiation (Figure 7); however, part of
374 this discrepancy is likely caused by errors in the observation data (Sonnenborg et al. 2013).
375 Simulations for night time conditions compare favourably to observations of both energy fluxes and
376 for both scenarios. As shown in Figure 6 the simulations for the validation period shows
377 comparable or better performance statistics for both fluxes as compared to the calibration period.

378 In the auto-calibration, simulations are compared to the same observed discharge data for
379 both HYP1 and HYP2 while the energy fluxes and albedos were adjusted to obtain energy balance
380 closure. This is reflected by differences in water balance components for the two hypotheses HYP1
381 and HYP2 both on catchment and local scales (Table 3). With a lower albedo in the HYP1 scenario
382 higher ET and therefore lower recharge and discharge are simulated at catchment scale. For the

383 agriculture grid cell the slightly higher ET for the HYP2 hypothesis can be ascribed to the lower
384 K_{sat} value. The significant difference in drainage is likely a function of higher groundwater
385 elevations in the HYP2 hypothesis. For forest and meadow the difference in albedo is reflected in
386 higher ET for HYP1.

387 The comparison of the performances of the full calibration and the scenarios with calibration
388 of the 1D models only and no calibration respectively is shown in figure 6. For discharge the
389 simulations with no calibration using default values is comparable to the results of the full
390 calibration whereas the 1D calibration is generally poorer. The most significant improvement in the
391 calibration approach is however seen for the LE and H energy fluxes where the mean root mean
392 square error (RMSE) and mean absolute error (MAE) statistics for the three sites is substantially
393 improved. The distributed simulations based on the values from the 1D calibration transferred to
394 catchment scale are generally of lower quality compared to the case where no calibration is carried
395 out. This, as opposed to using initial values using no calibration at all (default values), is because
396 neither input source includes parameters related to the distributed scale (e.g. related to discharge
397 and overland flow). Also, the extreme 1D mean RMSE statistics for H is due to the forest site which
398 was manually calibrated prior to the autocalibration (see above) and it does therefore not affect the
399 full 1D+2D calibration.

400

401 **5 Discussion**

402 We have presented an approach for a stepwise calibration of a distributed combined land
403 surface/hydrology model using observations of energy fluxes and discharge as calibration target. In
404 general the method proved effective. The validation period confirmed the performance statistics
405 from the calibration period and the simulations using a reduced calibration approach or no
406 calibration were generally less accurate.

407

408 **5.1 Energy and water balance**

409 As expected a key finding was that the choice of energy balance hypothesis has a major
410 impact on the resulting parameterization as well as on the energy and water balance results. The
411 lack of energy balance closure for flux measurements is therefore a great challenge when using such
412 measurements for calibrating distributed hydrological models. Energy balance closure is required
413 when flux measurements are used for inverse modelling and we investigated two hypotheses where
414 the error was attributed to either the measured energy fluxes (HYP1) or the measured net radiation
415 (HYP2).

416 Either of these two approaches may be applicable. Even though the eddy covariance method
417 is generally regarded as the best practical method for measuring energy fluxes, measurement
418 difficulties are well documented (Foken et al. 2006, Sun et al. 2008, Franssen et al. 2010, Ringgard,
419 2012, Stoy et al. 2013). A consistent deficit in measured LE fluxes have been suggested as an
420 explanation in the lack of energy balance closure (Sun et al. 2008) while on the other hand Foken et
421 al. (2006) suggested that low frequency turbulence structures cause errors in the flux measurements.
422 Also, measurement errors in H fluxes have been suggested, see (Mauder et al. 2008) and
423 Sonnenborg et al. (2013). The energy flux statistics (Figure 6) were better for the HYP2 hypothesis
424 possibly indicating that larger measurement errors are attributed to the energy fluxes compared to
425 radiation components. An additional contributing factor is the difference in the footprint of the flux
426 measurements reflecting conditions upstream of the wind direction and the support scale of the
427 radiation sensor.

428 Contrary to indications of flux measurement biases, estimates of ET based on eddy
429 covariance and soil moisture balances of the root zone compared well and surprisingly the highest
430 ET was seen for the eddy covariance method over a seven week period in May-June 2009 (Schelde

et al. 2011). Similarly, net radiation measurements from Foulum research station match the sum of LE, H and G fluxes better than for the agriculture, forest and meadow sites used in this study (Figure 3). Advection has also been suggested as a missing component in the energy balance suggesting that the measured energy fluxes may indeed be more reliable than anticipated (Leuning et al. 2012). Likewise, large scale eddies due to land surface heterogeneity have recently been suggested to make up a part of the energy imbalance (Stoy et al. 2013).

Snow processes are currently not considered the SWET land-surface model and this impacts the calibration results especially with regard to discharge. Even though the calibration period is relatively cold, little precipitation occurs on days with temperatures below 0 °C. Nevertheless, the snow melt related discharge peaks in Feb-Mar 2010 are clearly not reproduced (Figure 5).

5.2 Sensitivity, calibration and validation

The distinct differences between parameter sensitivities at the agriculture and forest sites compared to the meadow site are related to the water available for ET (Figure 8). At the agricultural and forest sites, complete soil saturation is rarely or never reached and there is a clear tendency for higher ET with lower soil moisture as this occurs during the summer months with a higher level of available solar energy. Soil parameters affecting available soil water are therefore crucial for determining the partitioning of energy fluxes at these sites. For the meadow site, located next to the river bank, saturated conditions are often reached (41% of the year for HYP2) and soil moisture levels are generally high. As a result the relation between root zone water and ET is less distinct. The high water availability at the meadow site therefore makes vegetation parameters substantially more important compared to soil parameters.

The choice of energy balance closure hypothesis, and therefore the energy available, is highly influential on which parameters are most sensitive especially for the agriculture and forest

sites but also to some extent for the meadow site. This is reflected in the sensitivities for the HYP1 and HYP4 hypotheses on one side and the HYP2 and HYP3 hypotheses on the other. This is consistent with the HYP1/HYP4 hypotheses being based on measured net radiation (averaged to 54, 67 and 56 W/m² in the calibration period for agriculture, forest and meadow) while the HYP2/HYP3 hypotheses are based on downscaled net radiation (40, 47 and 40 W/m² for the same sites).

The results of the sensitivity analysis and auto-calibration procedure naturally reflect the interplay between a vast number of parameters, assumptions regarding the energy balance terms, assumed relations between parameters for the individual soil layers, and the specific conditions that apply for the period subject to the analysis. These assumptions are required for reasons such as energy balance closure, calibration simplicity, data availability and focus of the study in question. For example, the parameter Rst_min is assumed constant in the present study whereas Ingwersen et al. (2011) obtained better simulations of LE and H based on the Noah LSM model using monthly values of Rst_min. Hou et al. (2012) related simulations of LE and H to parameter uncertainty in a study using the Community Land Model (CLM4) and documented substantial variations in the simulations of both fluxes (over 100 W/m²) in the summer months depending on the parameterization. The rather poor agreement between simulations and observations of H fluxes was likely due to observation errors. Separate auto-calibration runs were performed assessing forest heat fluxes based on forest parameterization alone with limited improvement and this is in line with the results by Sonnenborg et al. (2013).

5.3 Land use

Standard seasonal crop characteristics were used in this study and the actual crop rotation and management conditions at a given site were therefor not considered. This could lead to

479 discrepancies between the vegetation parameterization at the agricultural site particular around the
480 time of harvest and at the grass site due to irregular and undocumented cattle grazing. Possibly
481 more significant is the effect of the spatial distribution of crops derived from available county
482 average data, which may not reflect the actual distribution. This is the case both in terms of the
483 overall distribution, type and location of crops within the catchment. But it also affects the
484 evaluation of energy flux data from the agricultural site as the actual footprint may differ from the
485 simulated crop as also reported by Göckede et al. (2008).

486 The distributed MIKE SHE parameterization was performed by transferring the calibrated
487 parameters from the point scale setups, representing agriculture, meadow and forest, to the relevant
488 land surfaces within the catchment for subsequent sensitivity and auto-calibration analyses. For
489 agriculture, this procedure includes the tradeoff between using the calibrated parameter values
490 reflecting site specific conditions at the measurement site and using crop and soil specific
491 parameters from the Daisy model. However, the former was used since parameters were calibrated
492 under conditions of energy balance closure but also because of the statistical spatial distribution of
493 the Daisy modelled crop characteristics.

494

495 **6 – Conclusions**

496 In the present study we present a novel approach to calibrating a combined and distributed
497 hydrology/land-surface model. The approach first involves calibration of the land-surface model
498 component against measurements of energy fluxes from flux towers. Secondly, the distributed
499 hydrological model component, including unsaturated and saturated zone components, is calibrated
500 using the point scale parameterization as initial conditions and using stream flow and energy flux
501 measurements as the calibration targets. The method employs a meticulous literature inspection for
502 realistic initial and range of parameter values. Previous calibration efforts of SVAT and LSM

models with a hydrological focus have often used satellite data having certain measurement deficiencies, relied on previously point scale based parameterizations or used traditional hydrological variables such as discharge and hydraulic head. Modelling the highly interrelated and dynamical processes and variables in the entire water and energy budget from groundwater to lower atmosphere is challenging. Our results show that the proposed approach significantly improves the simulated energy balance components as compared to using default values or a simpler 1D calibration. The simulations were able to reproduce features across water and energy budgets taking into considerations measurement errors and lack of energy balance closure.

The calibration of the one dimensional models provided good insight to data quality and parameter sensitivity and served as a useful initial parameterization of the catchment scale simulations. Further, the sensitivities of parameters in the point scale analysis were highly affected by the surface type and more specifically the water availability as well as the choice of energy balance hypothesis. Similarly, the catchment model simulations showed that parameter sensitivities are largely determined by the choice of energy balance hypothesis, yet saturated hydraulic conductivity was the most sensitive parameter for both energy balance hypotheses. Despite likely errors in measured forest sensible heat fluxes, our results suggest that the measured energy fluxes are reliable and that the energy imbalance is likely caused by advection and large scale eddies rather than erroneous net radiation measurements.

7 - Acknowledgments

The present study was funded by a grant from the Danish Strategic Research Council for the project HYdrological Modelling for Assessing Climate Change Impacts at differeNT Scales (HYACINTS–www.hyacints.dk) under contract no: DSF-EnMi 2104-07-0008. The study is made possible

526 through a collaboration with the HOBE project (www.hobecenter.dk) funded by the Villum Kann
 527 Rasmussen Foundation. The data used in the study can be accessed through the first author.

528

529

530

531

532 **8 – References**

- 533 • Allerup, P., Madsen, H., Vejen, F., 1998. Standardværdier (1961-90) af Nedbørkorrektioner, Danish
 534 Meteorological Institute Technical Report 98-10, Denmark.
- 535 • Barr, A.G., van der Kamp, G., Black, T.A., McCaughey, J.H., Nesic, Z., 2012. Energy balance closure at
 536 the BERMS flux towers in relation to the water balance of the White Gull Creek watershed 1999–2009.
 537 Agric. Forest Meteorol. 153, 3–13. doi:10.1016/j.agrformet.2011.05.017.
- 538 • Beier, C., Gundersen, P., Hansen, K., Rasmussen, L., 1995. Experimental manipulation of water and
 539 nutrient input to a Norway spruce plantation at Klosterhede, Denmark. Plant Soil 168, 613–622.
- 540 • Beven, K.J., Franks, S.W., 2001. Functional similarity in landscape scale SVAT modelling. Hydrol.
 541 Earth Syst. Sc. 3, 85–93. doi:10.5194/hess-3-85-1999
- 542 • Beven, K., 2006. Searching for the Holy Grail of scientific hydrology: $Q_t = (S, R, ? t) A$ as closure.
 543 Hydrol. Earth Syst. Sc. Discussions 10, 609–618. doi:10.5194/hess-10-609-2006.
- 544 • Blasone, R. S., Madsen, H., Rosbjerg, D., 2007. Parameter estimation in distributed hydrological
 545 modelling: comparison of global and local optimisation techniques, Nord. Hydrol. 38(4–5), 451–476,
 546 doi:10.2166/nh.2007.024.
- 547 • Boulet, G., Kalma, J.D., Braud, I., Vauclin, M., 1999. An assessment of effective land surface
 548 parameterisation in regional-scale water balance studies. J. Hydrol. 217, 225–238.
- 549 • Breda, N.J.J., 2003. Ground-based measurements of leaf area index: a review of methods, instruments
 550 and current controversies. J. Exp. Bot. 54, 2403–2417. doi:10.1093/jxb/erg263

- 551 • Butts, M. B., Payne, J. T., Kristensen, M., Madsen, H., 2004. An evaluation of the impact of model
552 structure on hydrological modelling uncertainty for streamflow simulation, *J. Hydrol.* 298, 242–266,
553 doi:10.1016/j.jhydrol.2004.03.042.
- 554 • Butts, M., Drews, M., Larsen, M.A.D., Lerer, S., Rasmussen, S.H., Grooss, J., Overgaard, J., Refsgaard,
555 J.C., Christensen, O.B., Christensen, J.H., 2014. Embedding complex hydrology in the regional climate
556 system – Dynamic coupling across different modelling domains. *Adv. Water Resour.* 74, 166–184.
557 doi:10.1016/j.advwatres.2014.09.004
- 558 • Boegh, E., Poulsen, R.N., Butts, M., Abrahamsen, P., Dellwik, E., Hansen, S., Hasager, C.B., Ibrom, A.,
559 Loerup, J.-K., Pilegaard, K., Soegaard, H., 2009. Remote sensing based evapotranspiration and runoff
560 modeling of agricultural, forest and urban flux sites in Denmark: From field to macro-scale. *J. Hydrol.*
561 377, 300–316. doi:10.1016/j.jhydrol.2009.08.029
- 562 • Chen, F., Dudhia, J., 2001a. Coupling an Advanced Land Surface–Hydrology Model with the Penn
563 State–NCAR MM5 Modeling System. Part I: Model Implementation and Sensitivity. *Mon. Wea. Rev.*
564 129, 569–585. doi:10.1175/1520-0493(2001)129<0569:CAALSH>2.0.CO;2
- 565 • Choi, M., Kustas, W.P., Anderson, M.C., Allen, R.G., Li, F., Kjaersgaard, J.H., 2009. An
566 intercomparison of three remote sensing-based surface energy balance algorithms over a corn and
567 soybean production region (Iowa, U.S.) during SMACEX. *Agric. For. Meteorol.* 149, 2082–2097.
568 doi:10.1016/j.agrformet.2009.07.002
- 569 • Crow, P., 2005. The Influence of Soils and Species on Tree Root Depth, Environmental and Human
570 Sciences Division, Forest Research. ISBN 0-85538-679-7, United Kingdom.
- 571 • Dai, Z., Li, C., Trettin, C., Sun, G., Amatya, D., Li, H., 2010. Bi-criteria evaluation of the MIKE SHE
572 model for a forested watershed on the South Carolina coastal plain. *Hydrol. Earth Syst. Sc.* 14, 1033–
573 1046. doi:10.5194/hess-14-1033-2010.
- 574 • Demarty, J., Ottlé, C., Braud, I., Olioso, A., Frangi, J., Bastidas, L., Gupta, H., 2004. Using a
575 multiobjective approach to retrieve information on surface properties used in a SVAT model. *J. Hydrol.*
576 287, 214–236. doi:10.1016/j.jhydrol.2003.10.003

- 577 • DHI, 2010. AUTOCAL – Auto Calibration Tool, User Guide. MIKE by DHI Software, Hørsholm,
578 Denmark.
- 579 • Duan, Q., Gupta, V. K., Sorooshian, S., 1993. A shuffled complex evolution approach for effective and
580 efficient global minimization, *J Optimiz. Theory. Ap.*, 76, 501-521.
- 581 • Ewers, B.E., Oren, R., Johnsen, K.H., Landsberg, J.J., 2001. Estimating maximum mean canopy stomatal
582 conductance for use in models. *Can. J. Forest Res.* 31, 198–207. doi:10.1139/cjfr-31-2-198
- 583 • Foken T, Wimmer, F., Mauder, M., Thomas, C., Liebethal, C., 2006. Some aspects of the energy balance
584 closure problem, *Atmos. Chem. Phys.*, 6, 3381–3402, doi:10.5194/acp-6-4395-2006.
- 585 • Frank, A.B., Bittman, S., Johnson, D.A., 1996. Water relations of cool-season grasses. Cool-season
586 forage grasses, L.E. Moser et al. (ed.), *Agron. Monogr.*, 34, 127-164, ASA, CSSA, SSSA, Madison,
587 Wisconsin, USA.
- 588 • Franks, S.W., Beven, K.J., Quinn, P.F., Wright, I.R., 1997. On the sensitivity of soil-vegetation-
589 atmosphere transfer (SVAT) schemes: equifinality and the problem of robust calibration. *Agric. For.*
590 *Meteorol.* 86, 63–75. doi:10.1016/S0168-1923(96)02421-5
- 591 • Franks, S.W., Beven, K.J., Gash, J.H.C., 1999. Multi-objective conditioning of a simple SVAT model.
592 *Hydrol. Earth Syst. Sc. Discussions* 3, 477–488.
- 593 • Franssen, H.J.H., Stöckli, R., Lehner, I., Rotenberg, E., Seneviratne, S.I., 2010. Energy balance closure
594 of eddy-covariance data: A multisite analysis for European FLUXNET stations. *Agric. For. Meteorol.*
595 150, 1553–1567. doi:10.1016/j.agrformet.2010.08.005
- 596 • Graham, D. N., Butts, M.B., 2005. Flexible, integrated watershed modelling with MIKE SHE, In
597 *Watershed Models*, Eds. V.P. Singh & D.K. Frevert, 245-272, CRC Press. ISBN: 0849336090.
- 598 • Greve, M.H., Greve, M.B., Bøcher, P.K., Balstrøm, T., Breuning-Madsen, H., Krogh, L., 2007.
599 Generating a Danish raster-based topsoil property map combining choropleth maps and point
600 information. *Geografisk Tidsskrift-Danish Journal of Geography* 107, 1–12.
- 601 • Gryning, S.-E., Batchvarova, E., De Bruin, H.A.R., 2001. Energy balance of a sparse coniferous high-
602 latitude forest under winter conditions. *Bound.-Layer Meteor.* 99, 465–488.

- 603 • Göckede, M., Foken, T., Aubinet, M., Aurela, M., Banza, J., Bernhofer, C., Bonnefond, J.M., Brunet, Y.,
604 Carrara, A., Clement, R., Dellwik, E., Elbers, J., Eugster, W., Fuhrer, J., Granier, A., Grünwald, T.,
605 Heinesch, B., Janssens, I.A., Knohl, A., Koeble, R., Laurila, T., Longdoz, B., Manca, G., Marek, M.,
606 Markkanen, T., Mateus, J., Matteucci, G., Mauder, M., Migliavacca, M., Minerbi, S., Moncrieff, J.,
607 Montagnani, L., Moors, E., Ourcival, J.-M., Papale, D., Pereira, J., Pilegaard, K., Pita, G., Rambal, S.,
608 Rebmann, C., Rodrigues, A., Rotenberg, E., Sanz, M.J., Sedlak, P., Seufert, G., Siebicke, L., Soussana,
609 J.F., Valentini, R., Vesala, T., Verbeeck, H., Yakir, D., 2008. Quality control of CarboEurope flux data –
610 Part 1: Coupling footprint analyses with flux data quality assessment to evaluate sites in forest
611 ecosystems. *Biogeosciences* 5, 433–450. doi:10.5194/bg-5-433-2008
- 612 • Grimmond, C.S.B., Blackett, M., Best, M.J., Barlow, J., Baik, J.-J., Belcher, S.E., Bohnenstengel, S.I.,
613 Calmet, I., Chen, F., Dandou, A., Fortuniak, K., Gouvea, M.L., Hamdi, R., Hendry, M., Kawai, T.,
614 Kawamoto, Y., Kondo, H., Krayenhoff, E.S., Lee, S.-H., Loridan, T., Martilli, A., Masson, V., Miao, S.,
615 Oleson, K., Pigeon, G., Porson, A., Ryu, Y.-H., Salamanca, F., Shashua-Bar, L., Steeneveld, G.-J.,
616 Tombrou, M., Voogt, J., Young, D., Zhang, N., 2010. The International Urban Energy Balance Models
617 Comparison Project: First Results from Phase 1. *J. Appl. Meteorol.* 49, 1268–1292.
618 doi:10.1175/2010JAMC2354.1
- 619 • Gupta, H.V., Sorooshian, S., Yapo, P.O., 1998. Toward improved calibration of hydrologic models:
620 Multiple and noncommensurable measures of information. *Water Resour. Res.* 34, 751–763.
621 doi:10.1029/97WR03495
- 622 • Gupta, H.V., Bastidas, L.A., Sorooshian, S., Shuttleworth, W.J., Yang, Z.L., 1999. Parameter estimation
623 of a land surface scheme using multicriteria methods. *J. Geophys. Res.* (1984–2012) 104, 19491–19503.
- 624 • Hansen, S., Jensen, H. E., Nielsen, N. E., Svendsen H., 1990. Daisy: Soil-plant-atmosphere system
625 model. NPO National Agency of Environmental Protection Research Report No. A10. Copenhagen,
626 Denmark.
- 627 • Hansen, S., Jensen, H. E., Nielsen, N. E., Svendsen H., 1991. Simulation of nitrogen dynamics and
628 biomass production in winter wheat using the Danish simulation model DAISY. *Fert. Res.*, 27, 245–259.

- 629 • Hassan, Q.K., Bourque, C.P.-A., 2010. Spatial Enhancement of MODIS-based Images of Leaf Area
630 Index: Application to the Boreal Forest Region of Northern Alberta, Canada. *Remote Sens.* 2, 278–289.
631 doi:10.3390/rs2010278
- 632 • Hill, M.C., 1998. Methods and Guidelines for Effective Model Calibration. U.S. Geological Survey
633 Water-Resources Investigations Report 98-4005, USA.
- 634 • Hou, Z., Huang, M., Leung, L. R., Lin, G., Ricciuto, D. M., 2012. Sensitivity of surface flux simulations
635 to hydrologic parameters based on an uncertainty quantification framework applied to the Community
636 Land Model, *J. Geophys. Res.*, 117, D15108, doi:10.1029/2012JD017521.
- 637 • Hussein, A.S., 1999. Grass ET estimates using Penman-type equations in Central Sudan. *J. Irrig. Drain.*
638 *Eng.* 125, 324–329.
- 639 • Højberg, A. L., Trolborg, L., Stisen, S., Christensen, B. B. S., Henriksen, H. J., 2013. Stakeholder
640 driven update and improvement of a national water resources model, *Environ. Modell. Softw.*, 40, 202–
641 213. doi:10.1016/j.envsoft.2012.09.010
- 642 • Ingwersen, J., Steffens, K., Högy, P., Warrach-Sagi, K., Zhunusbayeva, D., Poltoradnev, M., Gäbler, R.,
643 Wizemann, H.-D., Fangmeier, A., Wulfmeyer, V., Streck, T., 2011. Comparison of Noah simulations with
644 eddy covariance and soil water measurements at a winter wheat stand. *Agric. For. Meteorol.* 151, 345–
645 355. doi:10.1016/j.agrformet.2010.11.010
- 646 • Iversen, B. V., Børgesen, C. D., Lægdsmand, M., Greve, M. H., Heckrath, G., Kjærgaard, C., 2011. Risk
647 Predicting of Macropore Flow using Pedotransfer Functions, Textural Maps, and Modeling. *Vadose Zone*
648 *J.*, 10, 1185–1195, doi:10.2136/vzj2010.0140.
- 649 • Jensen, K.H., Illangasekare, T. H., 2011. HOBE: A Hydrological Observatory. *Vadose Zone J.* 10, 1-7,
650 doi:10.2136/vzj2011.0006.
- 651 • Kelliher, F.M., Leuning, R., Raupach, M.R., Schulze, E.-D., 1995. Maximum conductances for
652 evaporation from global vegetation types. *Agr. Forest. Meteorol.* 73, 1–16. doi:10.1016/0168-
653 1923(94)02178-M

- 654 • Lagergren, F., Eklundh, L., Grelle, A., Lundblad, M., Mölder, M., Lankreijer, H., Lindroth, A., 2005. Net
655 primary production and light use efficiency in a mixed coniferous forest in Sweden. *Plant, Cell &*
656 *Environ.* 28, 412–423. doi:10.1111/j.1365-3040.2004.01280.x
- 657 • Lantinga, E.A., Nassiri, M., Kropff, M.J., 1999. Modelling and measuring vertical light absorption
658 within grass–clover mixtures. *Agr. Forest. Meteorol* 96, 71–83.
- 659 • Larsen, M. A. D., Thejll, P., Christensen, J. H., Refsgaard, J. C., Jensen, K. H., 2013. On the role of
660 domain size and resolution in the simulations with the HIRHAM region climate model, *Clim Dyn* 40,
661 2903–2918, doi:10.1007/s00382-012-1513-y.
- 662 • Larsen, M.A.D., Refsgaard, J.C., Drews, M., Butts, M.B., Jensen, K.H., Christensen, J.H., Christensen,
663 O.B., 2014. Results from a full coupling of the HIRHAM regional climate model and the MIKE SHE
664 hydrological model for a Danish catchment. *Hydrol. Earth. Syst. Sc.* 18, 4733–4749. doi:10.5194/hess-
665 18-4733-2014
- 666 • Lawrence, D.M., Oleson, K.W., Flanner, M.G., Thornton, P.E., Swenson, S.C., Lawrence, P.J., Zeng, X.,
667 Yang, Z.-L., Levis, S., Sakaguchi, K., Bonan, G.B., Slater, A.G., 2011. Parameterization improvements
668 and functional and structural advances in Version 4 of the Community Land Model. *J. Adv. Model. Earth*
669 *Syst.* 3, M03001. doi:10.1029/2011MS00045
- 670 • Lazzarotto, P., Calanca, P., Fuhrer, J., 2009. Dynamics of grass–clover mixtures—An analysis of the
671 response to management with the PROductive GRASSland Simulator (PROGRASS). *Ecol. Model.* 220,
672 703–724. doi:10.1016/j.ecolmodel.2008.11.023
- 673 • Lazzarotto, P., Calanca, P., Semenov, M., Fuhrer, J., 2010. Transient responses to increasing CO₂ and
674 climate change in an unfertilized grass–clover sward. *Clim. Res.* 41, 221–232. doi:10.3354/cr00847
- 675 • Leuning, R., van Gorsel, E., Massman, W.J., Isaac, P.R., 2012. Reflections on the surface energy
676 imbalance problem. *Agric. For. Meteorol.* 156, 65–74. doi:10.1016/j.agrformet.2011.12.002
- 677 • Li, H., Huang, M., Wigmosta, M.S., Ke, Y., Coleman, A.M., Leung, L.R., Wang, A., Ricciuto, D.M.,
678 2011. Evaluating runoff simulations from the Community Land Model 4.0 using observations from flux
679 towers and a mountainous watershed. *J. Geophys. Res.* 116, (D24120). doi:10.1029/2011JD016276

- 680 • Lindroth, A., Lagergren, F., Aurela, M., Bjarnadottir, B., Christensen, T., Dellwik, E., Grelle, A., Ibrom,
681 A., Johansson, T., Lankreijer, H., Launiainen, S., Laurila, T., MöLder, M., Nikinmaa, E., Pilegaard, K.,
682 Sigurdsson, B.D., Vesala, T., 2008. Leaf area index is the principal scaling parameter for both gross
683 photosynthesis and ecosystem respiration of Northern deciduous and coniferous forests. *Tellus B* 60,
684 129–142. doi:10.1111/j.1600-0889.2007.00330.x
- 685 • Madsen, H., 2003. Parameter estimation in distributed hydrological catchment modelling using
686 automatic calibration with multiple objectives. *Adv. Water Resour.* 26, 205–216.
- 687 • Mauder, M., Desjardins, R. L., Pattey, E., Gao, Z., van Haarlem, R., 2008. Measurement of the Sensible
688 Eddy Heat Flux Based on Spatial Averaging of Continuous Ground-Based Observations. *Bound.-Layer*
689 *Meteorol.* 128, 151–172. doi:10.1007/s10546-008-9279-9
- 690 • Maurer, E.P., Wood, A.W., Adam, J.C., Lettenmaier, D.P., Nijssen, B., 2002. A long-term hydrologically
691 based dataset of land surface fluxes and states for the conterminous United States. *J. Climate* 15, 3237–
692 3251.
- 693 • Mauser, W., Schädlich, S., 1998. Modelling the spatial distribution of evapotranspiration on different
694 scales using remote sensing data. *J. Hydrol.* 212, 250–267.
- 695 • Maxwell, R.M., Lundquist, J.K., Mirocha, J.D., Smith, S.G., Woodward, C.S., Tompson, A.F.B., 2011.
696 Development of a Coupled Groundwater–Atmosphere Model. *Mon. Weather Rev.* 139, 96–116.
697 doi:10.1175/2010MWR3392.1
- 698 • Mertens, J., Madsen, H., Feyen, L., Jacques, D., Feyen, J., 2004. Including prior information in the
699 estimation of effective soil parameters in unsaturated zone modelling. *J. Hydrol.*, 294, 251–269,
700 doi:10.1016/j.jhydrol.2004.02.011.
- 701 • Mertens, J., Madsen, H., Kristensen, M., Jacques, D., Feyen, J., 2005. Sensitivity of soil parameters in
702 unsaturated zone modelling and the relation between effective, laboratory and in situ estimates, *Hydrol.*
703 *Process.*, 19, 1611–1633, doi:10.1002/hyp.5591.

- 704 • Meyer, P. D., Rockhold, M. L., Wee, G. W., 1997. Uncertainty analyses of infiltration and subsurface
705 flow and transport for SDMP sites. Division of Regulatory Applications Office of Nuclear Regulatory
706 Research, U.S. Nuclear Regulatory Commission, Washington, USA.
- 707 • Moore, C., Doherty, J., 2005. Role of the calibration process in reducing model predictive error. *Water*
708 *Resour. Res.* 41, W05020. doi:10.1029/2004WR003501
- 709 • Nghi, V. V., Dung, D. D., Lam, D. T., 2008. Potential evapotranspiration estimation and its effect on
710 hydrological model response at the Nong Son Basin, *VNU Journal of Science, Earth Sciences*, 24, 213-
711 223.
- 712 • Olesen, J.E., Berntsen, J., Hansen, E.M., Petersen, B.M., Petersen, J., 2002. Crop nitrogen demand and
713 canopy area expansion in winter wheat during vegetative growth. *Eur. J. Agron.* 16, 279–294.
714 doi:10.1016/S1161-0301(01)00134-4
- 715 • Olesen, J.E., Hansen, P.K., Berntsen, J., Christensen, S., 2004. Simulation of above-ground suppression
716 of competing species and competition tolerance in winter wheat varieties. *Field Crop. Res.* 89, 263–280.
717 doi:10.1016/j.fcr.2004.02.005
- 718 • Overgaard, J., 2005. Energy-based land-surface modelling: new opportunities in integrated hydrological
719 modeling, Ph.D. Thesis, Institute of Environment and Resources, DTU, Technical University of
720 Denmark.
- 721 • Perry, D. A., 1994. *Forest Ecosystems*. The Johns Hopkins University Press, Maryland. 1. Ed. ISBN 0-
722 8018-4760-5.
- 723 • Pollacco, J.A.P., Mohanty, B.P., Efstratiadis, A., 2013. Weighted objective function selector algorithm for
724 parameter estimation of SVAT models with remote sensing data: Parameter Estimation for Svat Model.
725 *Water Resour. Res.* 49, 6959–6978. doi:10.1002/wrcr.20554
- 726 • Pokorný, R., Tomášková, I., Havráňková, K., 2008. Temporal variation and efficiency of leaf area index
727 in young mountain Norway spruce stand. *Eur. J. For. Res.* 127, 359–367. doi:10.1007/s10342-008-0212-
728 z

729 • Rautiainen, M., Heiskanen, J., Korhonen, L., 2012. Seasonal changes in canopy leaf area index and
730 MODIS vegetation products for a boreal forest site in central Finland, *Boreal Environ. Res.*, 17, 72-84.

731 • Ridler, M.E., Sandholt, I., Butts, M., Lerer, S., Mougin, E., Timouk, F., Kergoat, L., Madsen, H., 2012.
732 Calibrating a soil-vegetation-atmosphere transfer model with remote sensing estimates of surface
733 temperature and soil surface moisture in a semi arid environment. *J. Hydrol.* 436-437, 1-12.
734 doi:10.1016/j.jhydrol.2012.01.047

735 • Ringgaard, R., 2012. On variability of evapotranspiration - The role of surface type and vegetation.
736 Ph.D. Thesis, University Of Copenhagen, Department Of Geography and Geology, Denmark.

737 • Rosero, E., Yang, Z.-L., Wagener, T., Gulden, L.E., Yatheendradas, S., Niu, G.-Y., 2010. Quantifying
738 parameter sensitivity, interaction, and transferability in hydrologically enhanced versions of the Noah
739 land surface model over transition zones during the warm season. *J. Geophys. Res.* 115, D03106.
740 doi:10.1029/2009JD012035

741 • Sahoo, G.B., Ray, C., De Carlo, E.H., 2006. Calibration and validation of a physically distributed
742 hydrological model, MIKE SHE, to predict streamflow at high frequency in a flashy mountainous
743 Hawaii stream. *J. Hydrol.* 327, 94-109. doi:10.1016/j.jhydrol.2005.11.012

744 • Schelde, K., Ringgaard, R., Herbst, M., Thomsen, A., Friberg, T. and Sogaard, H., 2011. Comparing
745 Evapotranspiration rates estimated from Atmospheric Flux and TDR Soil Moisture Measurements,
746 *Vadose Zone J.*, 10, 78-83, doi:10.2136/vzj2010.0060.

747 • Schulze, E.-D., Kelliher, F.M., Korner, C., Lloyd, J., Leuning, R., 1994. Relationships among maximum
748 stomatal conductance, ecosystem surface conductance, carbon assimilation rate, and plant nitrogen
749 nutrition: a global ecology scaling exercise. *Ann. Rev. Ecol. Syst.* 629-660. doi:
750 10.1146/annurev.es.25.110194.003213.

751 • Shrestha, P., Sulis, M., Masbou, M., Kollet, S., Simmer, C., 2014. A Scale-Consistent Terrestrial Systems
752 Modeling Platform Based on COSMO, CLM, and ParFlow. *Mon. Weather Rev.* 142, 3466-3483.
753 doi:10.1175/MWR-D-14-00029.1

- 754 • Shuttleworth, W.J., Wallace, J.S., 1985. Evaporation from sparse crops-an energy combination theory.
755 Q.J.R. Meteorol. Soc. 111, 839–855. doi:10.1002/qj.49711146910
- 756 • Sonnenborg, T. O., Pang, B., Bruge, A., Christiansen, J. R., Stisen, S., Gundersen, P., 2013. Modeling of
757 evapotranspiration and groundwater recharge from forest. TR32-HOBE symposium, Bonn, Germany.
- 758 • Stisen, S., McCabe, M.F., Refsgaard, J.C., Lerer, S., Butts, M.B., 2011a. Model parameter analysis using
759 remotely sensed pattern information in a multi-constraint framework. J. Hydrol. 409, 337–349.
760 doi:10.1016/j.jhydrol.2011.08.030
- 761 • Stisen, S., Sonnenborg, T.O., Højberg, A.L., Trolborg, L., Refsgaard, J.C., 2011b. Evaluation of Climate
762 Input Biases and Water Balance Issues Using a Coupled Surface–Subsurface Model. Vadose Zone J. 10,
763 37. doi:10.2136/vzj2010.0001
- 764 • Stisen, S., Højberg, A. L., Trolborg, L., Refsgaard, J. C., Christensen, B. B. S., Olsen, M., Henriksen, H.
765 J., 2012. On the importance of appropriate precipitation gauge catch correction for hydrological
766 modelling at mid to high latitudes. Hydrol. Earth Syst. Sc., 16, 4157–4176, doi:10.5194/hess-16-4157-
767 2012.
- 768 • Stoy, P. C., Mauder, M., Foken, T., Marcolla, B., Boegh, E., Ibrom, A., Arain, M.A., Arneth, A., Aurela,
769 M., Bernhofer, C., others, 2013. A data-driven analysis of energy balance closure across FLUXNET
770 research sites: The role of landscape scale heterogeneity. Agric. For. Meteorol. 171, 137–152.
- 771 • Styczen, M., Hansen, S., Jensen, L. S., Svendsen, H., Abrahamsen, P., Børgesen, C. D., Thirup, C.,
772 Østergaard, H. S., 2004a. Standardopstillinger til Daisy-modellen. Vejledning og baggrund. Version 1.2,
773 april 2006. DHI Institut for Vand og Miljø, Denmark.
- 774 • Styczen, M., Hansen, S., Jensen, L. S., Svendsen, H., Abrahamsen, P., Børgesen, C. D., Thirup, C.,
775 Østergaard, H. S., 2004b. Appendix-samling, DHI Institut for Vand og Miljø, Denmark.
- 776 • Sun, G., Noormets, A., Chen, J., McNulty, S. G., 2008. Evapotranspiration estimates from eddy
777 covariance towers and hydrologic modeling in managed forests in Northern Wisconsin, USA, Agr.
778 Forest. Meteorol., 148, 257–267, doi:10.1016/j.agrformet.2007.08.010.

- 779 • Sun, Y., Hou, Z., Huang, M., Tian, F., Ruby Leung, L., 2013. Inverse modeling of hydrologic parameters
780 using surface flux and runoff observations in the Community Land Model. *Hydrol. Earth. Syst. Sc.* 17,
781 4995–5011. doi:10.5194/hess-17-4995-2013
- 782 • Thompson, J.R., Sørensen, H.R., Gavin, H., Refsgaard, A., 2004. Application of the coupled MIKE
783 SHE/MIKE 11 modelling system to a lowland wet grassland in southeast England. *J. Hydrol.* 293, 151–
784 179. doi:10.1016/j.jhydrol.2004.01.017
- 785 • Topping, C., Olsen, J., 2006. Vegetation growth simulation in ALMaSS. Danish Ministry of the
786 Environment report: Ukrudtsstriglingens effekter på dyr planter og ressourceforbrug, Appendix B,
787 Danish Ministry of the Environment, Copenhagen, Denmark.
- 788 • Twine, T.E., Kustas, W.P., Norman, J.M., Cook, D.R., Houser, Pr., Meyers, T.P., Prueger, J.H., Starks,
789 P.J., Wesely, M.L., 2000. Correcting eddy-covariance flux underestimates over a grassland. *Agric. For.*
790 *Meteorol.* 103, 279–300.
- 791 • van Genuchten, M. Th., 1980. A closed-form equation for predicting the hydraulic conductivity of
792 unsaturated soils, *Soil Sci. Soc. Am. J.*, 44, 892–898. doi:10.2136/sssaj1980.03615995004400050002x.
- 793 • Van der Keur, P., Hansen, S., Schelde, K., Thomsen, A., 2001. Modification of DAISY SVAT model for
794 potential use of remotely sensed data. *Agric. For. Meteorol.* 106, 215–231.
- 795 • Wang, Q., Tenhunen, J., Falge, E., Bernhofer, C.H., Granier, A., Vesala, T., 2004. Simulation and scaling
796 of temporal variation in gross primary production for coniferous and deciduous temperate forests. *Glob.*
797 *Change Biol.* 10, 37–51. doi:10.1046/j.1529-8817.2003.00716.x.
- 798 • Wilson, K., Goldstein, A., Falge, E., Aubinet, M., Baldocchi, D., Berbigier, P., Bernhofer, C., Ceulemans,
799 R., Dolman, H., Field, C., others, 2002. Energy balance closure at FLUXNET sites. *Agric. For. Meteorol.*
800 113, 223–243.
- 801 • Wösten, J. H. M., Lilly, A., Nemes, A., Le Bas, C., 1999. Development and use of a database of
802 hydraulic properties of European soils, *Geoderma*, 90, 169–185, doi:10.1016/S0016-7061(98)00132-3.

- 803 • Xevi, E., Christiaens, K., Espino, A., Sewnandan, W., Mallants, D., Sørensen, H., Feyen, J., 1997.
- 804 Calibration, validation and sensitivity analysis of the MIKE-SHE model using the Neuenkirchen
- 805 catchment as case study. *Water Resour. Manag.* 11, 219–242.
- 806 • Zhou, M.C., Ishidaira, H., Hapuarachchi, H.P., Magome, J., Kiem, A.S., Takeuchi, K., 2006. Estimating
- 807 potential evapotranspiration using Shuttleworth–Wallace model and NOAA-AVHRR NDVI data to feed
- 808 a distributed hydrological model over the Mekong River basin. *J. Hydrol.* 327, 151–173.
- 809 doi:10.1016/j.jhydrol.2005.11.013
- 810 • Zweifel, R., Böhm, J.P., Häsler, R., 2002. Midday stomatal closure in Norway spruce—reactions in the
- 811 upper and lower crown. *Tree Physiol* 22, 1125–1136.
- 812
- 813
- 814

Figure 1. Skjern catchment (Denmark). Locations of the flux tower and discharge sites and land use map (land use map from Jensen and Illangasekare (2011)).

Figure 2. Flow chart of the calibration process.

815

Figure 3. Measured radiation and energy flux components at the three Skjern catchment sites for the years 2009 and 2010, simulated components by the HIRHAM regional climate model, and measurements for year 2009 from an agricultural research station in Foulum located approx. 50 km north of the agriculture and forest sites. Yearly average values for each radiation and energy flux component is given in the legend. Measurements from the agricultural station in 2009 are bracketed due to extensive gap filling in this period.

Figure 4. Results of the sensitivity analyses for the individual sites and the distributed setup. For the distributed setup only the 20 most sensitive parameters are shown. The y-axis represents relative sensitivity in relation to the most sensitive parameter.

Figure 5. Observed and simulated daily and accumulated discharge at three gauging stations based on two energy balance hypothesis setups for the calibration and validation periods.

Figure 6. Catchment scale simulation statistics. Root mean square error (RMSE) and mean absolute error (MAE) statistics for discharge, latent heat flux (LE) and sensible heat flux (H) for the two energy balance hypotheses and for both the calibration and validation period (RMSE only).

Figure 7. Example of model simulated LE and H energy fluxes for the distributed case and for the two energy balance hypotheses in the calibration period. Un-scaled and scaled observations are also shown. The data represent a summer period June 1-11, 2010 with cloudless conditions from June 1-5 and varying global radiation from June 6-11. Lines of the same colour are comparable.

Figure 8. Daily values for plant transpiration and soil evaporation as a function of the average root zone water content at the three sites in the calibration period for HYP2 and the corresponding soil field capacity (pF 2) and saturation levels (dotted lines).

Table 1. Point scale parameterization.

Initial parameter values, parameter range for the sensitivity and optimization analyses for the three sites, and the resulting range for the four energy balance hypotheses. A selection of literature used to provide initial and range of parameter values (primary references listed first next to each parameter): 1) Lagergren et al. (2005), 2) Boulet et al. (1999), 3) Bøgh et al. (2009), 4) Chen and Dudhia (2001a), 5) Rautiainen et al. (2012), 6) Crow (2005), 7) Gryning et al. (2001), 8) Lindroth et al. (2008), 9) Van der Keur et al. (2001), 10) Overgaard (2005), 11) Perry (1994), 12) Hansen et al. (1991), 13) Hussein (1999), 14) Lazzarotto et al. (2010), 15) Topping and Olesen (2006), 16) Nghi et al. (2008), 17) Olesen et al. (2002), 18) Olesen et al. (2004), 19) Beier et al. (1995), 20) Bréda (2003), 21) Hassan and Borque (2010), 22) Pokorný et al. (2008), 23) Stisen et al. (2011a), 24) Lantinga et al. (1999), 25) Zweifel et al. (2002), 26) Lazzarotto et al. (2009), 27) Ingwersen et al. (2011), 28) Kelliher et al. (1995), 29) Zhou et al. (2006), 30) Wang et al. (2003), 31) Ridler et al. (2012), 32) Sahoo et al. (2006), 33) Xevi et al. (1997), 34) Dai et al. (2010), 35) Ewers et al. (2001), 36) Frank et al. (1996), 37) Schulze et al. (1994) and 38) Stisen et al. (2011b).

* Seasonal variation included. If brackets only some of the sites include seasonality (A; agriculture, M; meadow). With seasonality, the values are from mid-summer.

^S Parameter only included only in the sensitivity analysis.

Initial parameter value based on ^O observations, ^{SIM} simulated values by Daisy model and ^{VG} Van Genuchten parameter derived from pedotransfer function. Parameter values are considered for the A, B and C horizons and the parameter ranges are derived from Meyer et al (1997).

	Agriculture			Forest			Meadow		
Parameter	Initial value	Range	Calibrated values (hypothesis range)	Initial value	Range	Calibrated values (hypothesis range)	Initial value	Range	Calibrated values (hypothesis range)
Leaf area index* (m ² /m ²)	4.6 (SIM,9,29,37,27,15)	2.56-6.64	2.69-3.35	4.8 (O,19,1,5,29,37,20,3,7,8,16,21,2,2,30)	3.6-10.2	3.15-7.07	4.5 (15,26,29,37)	2.5-6.66	2.74-3.08
Root depth*(A, M) (m)	0.78 (SIM,29)	0.2-0.8	-	1.5 (6,29,3)	1-2	1.29-1.95	0.6 (SIM,3,29)	0.4-0.8	-
Minimum stomatal resistance (Rst_min) (s/m)	90 (9,28,29,37,23,27,4)	50-200	100-194	125 (23,28,25,29,35,37,4,16)	65-258	188-236	92.5 (2,28,29,36,37,23,4)	55-250	212-241
Extinction coefficient	0.53 (23,17,18,15,12)	0.4-0.85	0.47-0.66	0.46 (1,23,20,11)	0.15-0.52	-	0.45 (15,26,23,14,13,2,4)	0.25-0.75	0.26-0.45
Leaf width (m)	0.01 (9,29)	0.005-0.3	0.05-0.26	0.0025 (29)	0.000-5-0.3	0.01-0.05	0.01 (9,29)	0.005-0.3	0.01-0.03
Vegetation height*(A, M) (m)	0.78 (SIM)	0.51-1.03	0.55-0.98	17.5 (O, 3)	10-22.5	11.1-19.8	0.3 (3)	0.11-0.49	0.04-0.08
Roughness length*(A, M) (m)	0.03 (10,29,31)	0.007-5-0.12	-	0.03 (10,29,31)	0.007-5-0.12	-	0.03 (10,29,31)	0.007-5-0.12	-
Interception coefficient (mm)	0.05 (29,31,32,33,34)	0.01-0.2	0.02-0.13	0.05 (29,31,32,33,34)	0.01-0.2	0.01-0.15	0.05 (29,31,32,33,34)	0.01-0.2	0.05-0.16
Root shape factor	1 (31,32,33)	0.2-4	0.24-3.66	1 (31,32,33)	0.2-4	0.02-0.07	1 (31,32,33)	0.2-4	-
Detention storage (mm)	10 (34,38)	5-100	-	10	5-100	11.5-46-5	10	5-100	49.4
Initial water content ^s (m ³ /m ³)	0.2	0.1-0.4	-	0.2	0.1-0.4	-	0.2	0.1-0.4	-
Van Genuchten α (cm ⁻¹)	0.062/0.082/0.085 (VG)	0.008-7-0.128	0.01-0.1	0.062/0.082/0.085 (VG)	0.008-7-0.128	0.01-0.02	0.048/0.058/0.056 (VG)	0.004-5-0.11	-
Van Genuchten n	1.445/1.58/1.72 (VG)	1.25-1.88	-	1.445/1.58/1.72 (VG)	1.25-1.88	-	1.3/1.35/1.32 (VG)	1.16-1.65	12.2-14.9
Saturated hydraulic conductivity (m s ⁻¹)	1.4E-5/1.04E-5/1.12E-5 (VG)	3.9E-7-1.86E-4	3.9E-7 - 5.5E-7	1.4E-5/1.04E-5/1.12E-5 (VG)	3.9E-7-1.86E-4	4E-7 - 4.24E-7	6.86E-6 (VG)	3.49E-9-1.34E-4	7.6E-7-4.9E-6
Residual water	1.0E-3/1.0E-3/1.0E-3 (VG)	0-0.028	-	1.0E-3/1.0E-3/1.0E-3 (VG)	0-0.028	-	0.02/0.02/0.02 (VG)	0.017-0.11	-

Comment [madla1]: We noticed that, by mistake, leaf width results had been copied to here.

Parameter	Distribution type	Range	HYP1		HYP2	
		HYP1 and HYP2	Initial value	Calibrated value	Initial value	Calibrated value
Leaf area index* (m ² /m ²)	Agriculture	2.56-6.64	2.97	5.66	2.69	
Root depth*(A,M) (m)		0.2-0.8	0.78		0.78	
minimum stomatal resistance (Rst_min) (s/m)		50-200	136		194	
Extinction coefficient		0.4-0.85	0.66		0.47	
Leaf width (m)		0.005-0.3	0.05		0.25	0.23
Vegetation height*(A,M) (m)		0.51-1.03	0.8		0.98	
Roughness length*(A,M) (m)		0.05-0.13	0.08 (1)		0.098 (1)	
Leaf area index* (m ² /m ²)	Forest	3.6-10.2	3.84	7.41	3.15	3.12
Root depth*(A,M) (m)		1-2	1.95		1.34	
minimum stomatal resistance (Rst_min) (s/m)		65-258	188	244	193	237
Extinction coefficient		0.15-0.52	0.46	0.16	0.46	0.22
Leaf width (m)		0.0005-2	0.04	1.93	1	0.85
Vegetation height*(A,M) (m)		10-22.5	19.8	13.2	11.1	10.6
Roughness length*(A,M) (m)		1-2.25 (1)	0.2	0.014	0.11	0.04
Leaf area index* (m ² /m ²)	Meadow	2.5-6.66	2.74		2.73	3.95
Root depth*(A,M) (m)		0.4-0.8	0.6		0.6	
minimum stomatal resistance (Rst_min) (s/m)		55-250	247		238	
Extinction coefficient		0.25-0.75	0.26		0.45	
Leaf width (m)		0.005-0.3	0.02		0.01	0.0085
Vegetation height*(A,M) (m)		0.11-0.49	0.27		0.15	
Roughness length*(A,M) (m)		0.011-0.049 (1)	0.007		0.004	
Interception coefficient (mm)	Global	0.01-0.2	0.13		0.07	0.148
Root shape factor		0.2-4	0.89	0.46	3.66	0.39
Detention storage		5-100	40		40	95
Night cloudiness		0.01-0.99	0.5	0.0136	0.5	
Drainage time constant (s ⁻¹)		6.50E-08-5.5E-7 (4)	1.02E-07		1.02E-07	
Leakage coefficient (m/s)		1.38E-7-1.38E-5 (2,3)	1.38E-06	1.17E-6	1.38E-06	
Overland Manning number (m ^{1/2} s ⁻¹)		2-15 (2,3)	7.5		7.5	
River manning number (m ^{1/2} s ⁻¹)		18.75-31.25 (3)	25		25	
Soil heat capacity reduction		0.01-0.99	0.5	0.48	0.5	0.13
Soil heat conductivity reduction		0.01-0.99	0.5	0.0121	0.5	0.039
Van Genuchten α (cm ⁻¹)	By soil type (values for top layer)	0.009-0.128	0.0129	0.093	0.126	
Van Genuchten n		1.2459-1.8842	1.27	1.7	1.3	1.51
Saturated hydraulic conductivity (K_sat) (m s ⁻¹)		3.9E-7-1.86E-4	1.40E-05	1.01E-5	4.00E-07	2.02E-6
Residual water content (m3/m3)		0-0.0278	0		0	
Saturated water content (m3/m3)		0.247-0.543	0.53		0.537	

Table 3. Catchment scale simulation water balance. Water balance components for the total catchment as well as values from the grid cells of the three flux tower sites extracted from the distributed catchment. The total catchment albedos are area weighted values and the observed ET values are in brackets.

	Total catchment		Agri.		Forest		Meadow	
	HYP1	HYP2	HYP1	HYP2	HYP1	HYP2	HYP1	HYP2
Albedo	0.18	0.35	0.19	0.32	0.08	0.40	0.19	0.42
Precipitation (mm)	1094	1094	1119	1119	1007	1007	991	991
Evapotranspiration (mm)	481	454	424 (407)	434 (407)	561 (519)	460 (519)	584 (440)	539 (440)
Canopy Evap. (mm)	192	133	165	83	278	118	245	260
Recharge (mm)	513	579	708	700	151	383	412	468
Discharge (mm)	412	453	0	0	0	0	366	420
Overland flow (mm)	11	11	0	0	0	0	0	0
Pumping (mm)	55	50	104	104	0	0	0	0
Baseflow to river (mm)	205	216	0	0	0	0	43	40
Drain to river (mm)	207	237	30	164	0	0	323	380

Calibration of a distributed hydrology and land surface model using energy flux measurements

Morten A. D. Larsen^{1*}, Jens C. Refsgaard², Karsten H. Jensen³, Michael B. Butts⁴, Simon Stisen² and Mikkel Møllerup⁵.

1 - Technical University of Denmark, Department of Management Engineering, Frederiksborgvej 399, 4000 Roskilde, Denmark

2 - Geological Survey of Denmark and Greenland, Øster Voldgade 10, 1350 Copenhagen, Denmark.

3 - University of Copenhagen, Department of Geosciences and Natural Resource Management, Øster Voldgade 10, 1350 Copenhagen, Denmark.

4 - DHI, Agern Alle 5, DK 2970, Hørsholm, Denmark

5 - The Danish Road Directorate, Guldalderen 12, 2640 Hedehusene.

* - Corresponding author: madla@dtu.dk/004525119895

Keywords: hydrology/land surface modelling; calibration; water and energy fluxes; evapotranspiration; energy closure imbalance

1 Abstract

In this study we develop and test a calibration approach on a spatially distributed groundwater-surface water catchment model (MIKE SHE) coupled to a land surface model component with particular focus on the water and energy fluxes. The model is calibrated against time series of eddy flux measurements from three sites of different land surface type (agriculture, forest and meadow) and river discharge data from the 2500 km² Skjern River catchment in Denmark. The approach includes initial calibrations of three one-dimensional models representing the three land surface types ~~and~~ using the flux measurements for calibration. This step provides

initial values for the subsequent modelling and calibration at catchment scale. To test the validity of the approach, two additional catchment scale distributed simulations were performed with no calibration and only calibration of the one-dimensional models, respectively. In addition, a subsequent validation period was simulated. A mean energy closure imbalance of 20% was seen for the three sites. For the distributed simulations, the energy imbalance was accounted for by two energy balance closure hypotheses ascribing the error to either energy fluxes or net radiation. In general, the distributed calibration approach improved model results substantially compared to using default values (no calibration) or calibration of the one-dimensional models only. For the distributed model simulations, the assumption regarding the energy balance closure had a substantial impact on the parameter sensitivities and on the simulated discharge and energy balance. During calibration, the simulation with corrected energy fluxes showed better performance on discharge than the simulation with corrected net radiation whereas the reverse was true for the validation period. Regarding energy fluxes, the simulation with corrected net radiation was superior in both the calibration and validation period.

40

41 **2 Introduction**

Water and energy fluxes between land surface and atmosphere are important components of atmospheric and hydrological processes. These fluxes can be quantified by the use of land surface models (LSM) or soil-vegetation-atmosphere-transfer models (SVAT). The calculation of e.g. evapotranspiration in SVATs and LSMs is based on solving the energy and radiation equations often on a sub-daily basis and they therefore differ from the less physically stringent schemes often used in many traditional hydrological models which are based on potential evapotranspiration. LSMs, originating from atmospheric sciences, include spatially distributed, often large scale descriptions of land surface processes. Examples include the Noah model (Rosero et al. 2010) and the CLM model

(Lawrence et al. 2011). LSMs are typically coupled with or forced by atmospheric models and have recently been included in fully coupled climate-hydrology models (Maxwell et al. 2011, Shrestha et al. 2014). SVATs, originating from soil and hydrological sciences, are one-dimensional descriptions typically used for small-scale descriptions linked with soil water flow models (Mauser and Schädlich 1998, Ridler et al. 2012). When included in spatially distributed hydrological models they possess the potential for providing improved evapotranspiration descriptions and enable hydrological catchment models to better utilise remote sensing data to force and constrain hydrological models (Stisen et al. 2011a). SVATs have also recently been included in fully coupled climate-hydrology models (Butts et al. 2014, Larsen et al. 2014). LSMs and SVATs linked to spatially distributed hydrological models are basically similar, and hence we shall in the following refer to both of them as SVAT models.

Assessment of parameter values is critical for the use of SVAT models and an essential challenge is related the vast number of parameters often seen in this type of models. Franks et al. (1997, 1999), Beven and Franks (1999) and Gupta et al. (1999) all highlight the high uncertainty in the predictive capabilities of multi-parameter SVATs due to equifinality. Yet; Franks et al. (1997, 1999) still show good results in terms of reproducing point site flux measurements from the FIFE area in Kansas, USA, and in the Amazon area in Brazil. The added value of a multi-criteria approach as opposed to a single criterion method is confirmed by Gupta et al. (1999) and Demarty et al. (2004). Pollacco et al. (2013) apply an objective function weighing algorithm based on the uncertainties related to remote sensing based surface soil moisture and evapotranspiration calibration variables. Currently no explicit guidelines have been developed on calibrating complex and distributed SVAT and hydrology models.

Parameter estimation for hydrological models is traditionally performed by use of calibration where parameter values are modified to obtain best possible fit between model

74 simulations and observed target data. While calibration was previously often performed manually
75 by a trial-and-error approach, parameter optimisation by inverse modelling is now the method of
76 choice (Gupta et al. 1998, Madsen 2003, Moore and Doherty 2005). An example is the study by Sun
77 et al. (2013) where inverse calibration based on Monte Carlo-Bayesian techniques was used for
78 calibrating a model both against energy fluxes at point scale and runoff at catchment scale (4.9
79 km²). In Ingwersen et al. (2011) inverse calibration was used to simulate the water and energy
80 budget for a winter wheat stand at plot scale. Similarly Ridler et al. (2012) utilized inverse
81 techniques for calibrating the combined MIKE SHE/SWET model to simulate energy fluxes at point
82 scale in Mali.

83 A particular problem related to calibration of SVAT models is that observations of water and
84 energy fluxes are usually not available from operational monitoring networks but only from a few
85 research stations and often for short periods (Wilson et al. 2002, Franssen et al. 2010, Leuning et al.
86 2012). In addition, energy flux data are known to often have problems with energy balance closure
87 which severely hampers parameter optimisation by inverse modelling, as a SVAT model per
88 definition assumes a closed energy balance (Twine et al. 2000, Choi et al. 2009) and a failure to
89 meet this demand can result in significant biases in long term climate model simulations
90 (Grimmond et al. 2010). Also, the lack of measured energy balance closure will yield an erroneous
91 parameterization when the fluxes are used for the calibration of a hydrological model. Therefore
92 certain assumptions need to be made to account for the lack of closure. To accommodate this,
93 Beven (2006) suggested creating artificial hypotheses to provide closure.

94 Catchment water balances are linked to energy balances, because the latent
95 energy/evapotranspiration appears as a key element in both balances. The observed catchment
96 runoff and the catchment water balance assessed by hydrological models hence include important
97 information also on the energy balance. On a catchment scale (603 km²) Barr et al. (2012) used

~~distributed flux tower measurements of evapotranspiration against measured precipitation and discharge for a residual analysis on water balance closure concluding a 15% lack of energy flux closure compared to the measured net energy. For catchment scale (205 km²) model calibration, Li et al. (2011) used both runoff and energy fluxes for model calibration. The CLM4 model was modified to include a runoff scheme and calibration for a 205 km² catchment was performed manually against, to evaluate both runoff and at the same time considering energy fluxes. Similarly, operating on a regional to continental scale Maurer et al. (2002) simulated energy flux components while the model was manually calibrated only against runoff.~~

The objectives of the present study is to develop and test a methodology for calibrating and assessing parameters of a SVAT model linked to a spatially distributed hydrological model by using observations of both energy fluxes and catchment runoff. A comprehensive literature study was carried out to obtain feasible initial values and range of variation for parameters for the considered land surface types. The impact of energy imbalance is of particular emphasis and we analyse to which extent inclusion of discharge observations in the calibration process will improve the model performance and robustness.

3 Methodology

3.1 Study area and data

The Skjern catchment (2500 km²) is located in the western part of the Jutland peninsula, Figure 1. The catchment is dominated by sandy soils generated by glacial outwash plains from the last glacial period Weichsel and intersected by older till deposits from the previous glacial period Saalian (Greve et al. 2007). The topography reaches 130 m above sea level in the eastern part of the catchment and the Skjern River flow into Ringkøbing fjord at sea level to the west. The yearly average precipitation for the catchment is 940 mm for the period 2000-2009 based on direct

122 measurements. When corrected for undercatch using standard monthly correction factors (Allerup et
123 al. 1998) the average precipitation amounts to 1130 mm. In the same period the mean annual
124 temperature is 9.3 °C and the mean monthly temperatures range between 2.1 and 17.3 °C. Inside the
125 catchment flux towers are placed at the three predominant surface types; agriculture (61%),
126 meadow/grass (24%) and forest (13%), Figure 1. At all sites measurements of short-, long-wave and
127 net radiation components; latent (LE), sensible (H) and soil heat fluxes (G); soil water content;
128 precipitation; air temperature; wind speed; and water table levels have been carried out since late
129 2008. Measurements of radiation and energy fluxes are based on standard methods. Radiation
130 components are measured using a NR01 Hukseflux radiometer (www.hukseflux.com), LI-COR
131 eddy covariance equipment is used for measuring LE fluxes, Gill sonic anemometers for measuring
132 H fluxes, and Hukseflux plates for measuring G fluxes.

133 The energy flux data used in the study have undergone quality control as part of the
134 processing (Ringgard, 2012) (Step 1.3, Figure 2). Inaccurate observations caused by e.g. low
135 turbulence condition were replaced by data representing similar conditions. Replacement of data
136 was thus for periods with low energy fluxes and therefore this source of uncertainty is expected to
137 be of minor significance. Individual data points clearly outside the expected range at the time of day
138 and season were considered as outliers and removed- (equal to 0.2% on average between LE, H and
139 the three stations weighted relative the areal share). For two periods July 21-August 16 and August
140 24-October 28, 2009, no flux measurements were available from the agricultural site and data were
141 replaced from the forest site. As these periods are mostly placed in the spin-up period (see below)
142 the calibration results are not expected to be significantly affected.

143

144 3.2 Modelling system and setup

145 This study uses the spatially distributed MIKE SHE hydrological modelling system capable
146 of including all key hydrological processes such as ET, channel flow, overland flow, unsaturated
147 flow, saturated flow as well as irrigation and drainage (Graham and Butts 2005). The land surface
148 model SWET component (Overgaard, 2005) is used in the analysis. SWET is based on the
149 Shuttleworth-Wallace model (Shuttleworth and Wallace 1985). It considers vegetation and energy
150 balance processes in a two-layer system and is extended to include energy fluxes from ponded
151 water and interception storage. Models are constructed for both the three local measurement sites
152 (1D representation) and for the entire catchment (Figure 1).

153 The 1D models simulate energy fluxes and vertical unsaturated flow based on Richards'
154 equation. The SWET model is driven by 30 min climatic observations of precipitation, air
155 temperature, wind speed, net radiation, surface air pressure and relative humidity. Measured water
156 table elevations are specified as lower boundary condition. As opposed to the fully distributed
157 model application overland flow, river flow and groundwater flow are not considered. Relevant to
158 both the 1D and distributed analyses, the SWET land-surface module does not consider snow
159 accumulation and melting. Initial values for root depth and vegetation height applicable for the 1D
160 simulations of the agricultural and meadow sites were based on estimates from model simulations
161 for relevant soil type and management conditions using the vegetation model Daisy (Styczen et al.
162 2004a). Since the footprint of the flux tower at the agricultural site was influenced by several crop
163 types, the vegetation height and root depth were based on average simulations for winter- and
164 spring cereals. The observational data for leaf area index (LAI), another important crop parameter,
165 was inconsistent, and the seasonal variation of this parameter was therefore derived by combining
166 the observed seasonal trends and the simulation results by the Daisy model. The initial values for
167 soil parameters for each site were derived from the HYPRES pedotransfer function (Wösten et al.
168 1999). Specifically, the Van Genuchten parameters α and n (van Genuchten, 1980) as well as

169 saturated hydraulic conductivity, residual- and saturated water content were estimated from soil
170 texture, organic matter and bulk density. The soil texture data were retrieved from grid values from
171 a distributed soil map of 250 m resolution in the A horizon (0-30 cm) and 500 m resolution in B and
172 C horizons (30-80 cm and below 80 cm) (Styczen et al. 2004b, Greve et al. 2007, Iversen et al.
173 2011). For the sensitivity and optimization analyses the soil parameter bounds were defined by
174 calculating the 90% confidence intervals of variation ranges from Meyer et al. (1997) for soils of
175 similar texture as for the three field sites. These soil types include sand, loamy sand and sandy loam
176 for the agriculture and forest site roughly corresponding to JB1 soil (coarse sand) in the Danish soil
177 classification system (Greve et al. 2007, www.djfgeodata.dk). Due to the lack of agreement on soil
178 type at the meadow site between site specific soil retention data and available soil maps the 90%
179 confidence intervals for the meadow site is based on a wider range of soil types from loamy sand to
180 clay loam (Meyer et al. 1997). The discrepancy of the data is most likely due to highly
181 heterogeneous soils caused by shifting alluvial deposits from the nearby Skjern River. In the
182 parameterization the seasonal patterns of vegetation characteristics as induced by both climate and
183 management practice were kept constant whereas the respective amplitudes were calibrated by a
184 single factor for each parameter. The annual sequence of these ratios was found by balancing model
185 simulations by Daisy, relevant literature values (Table 1) and occasional on-site measurements of
186 LAI and vegetation height. Similarly, the relation between the parameter values in the three vertical
187 soil type horizons were kept constant implying that the individual parameters for the A, B and C
188 horizon were shifted by the same factor for each grid cell. By introducing factors between
189 parameters in space and time the number of parameters to be optimized is reduced.

190 The MIKE SHE model for catchment scale is based on the Danish national water resources
191 model (DK-model) (Stisen et al. 2012, Højberg et al. 2013). As opposed to the DK-model the
192 present model includes the SWET land-surface model and the parameterization of this model is

193 partly based on the work by Stisen et al. (2011a). The DK model has a 500 m resolution and
194 includes a detailed river network. A maximum time step of 1 hour is used for overland, unsaturated
195 and saturated flow. The MIKE 11 open channel river model component utilizes 3616 cross sections
196 in 100 river branches and uses a 30 min time step. For precipitation exceeding 2 mm per time step
197 an automatic reduction in time step takes place. The input for the catchment scale SWET model is
198 hourly values of the same climatic variables as for the 1D models. These values are obtained by thin
199 plate spline interpolation of climate station data (Stisen et al. 2011a) to a resulting grid in 2 km
200 resolution for all variables except precipitation used in 500 m resolution. Precipitation input is
201 based on interpolation of daily rain gauge data using kriging and dynamically corrected for
202 undercatch. ~~Simulated irrigation is subsequently added to precipitation.~~Hereafter, simulated
203 irrigation is added to the precipitation input file. The simulated irrigation is calculated from the root
204 zone deficit and a demand function based on well locations, filter depths, annual abstractions and
205 demand area information (Stisen et al. 2011b). The agricultural crop distribution was developed
206 from statistical data, where the various crops were grouped in four classes with different growth
207 characteristics: spring sown cereals, winter sown cereals, grass/clover and maize. The crop classes
208 were distributed without georeferencing due to lack of data. Forest vegetation parameters were
209 based on relevant literature and observations. A total of 36 parameters were analysed in the
210 sensitivity analysis. As the calibration is targeted towards the energy fluxes no sensitivity and
211 calibration analyses are performed on the saturated zone parameterization which is already well
212 calibrated as a part of the DK-model (Stisen et al. 2012, Højberg et al. 2013).

213 To generate proper initial conditions for soil moisture in the 1D simulations a spin-up period
214 of 5-10 months prior to the calibration period was used. The spin-up periods were decided by data
215 availability as measurements started in April 2009 for the agriculture and meadow sites and
216 December 2008 for the forest site. The distributed model involves a considerable increase in

217 computation time compared to the 1D setups and a spin-up period of 3 months was therefore used.
218 Groundwater quasi steady-state was reached by looping simulations in 3-year runs each time using
219 the resulting groundwater heads as initial conditions for the subsequent simulation. Three loops
220 were required to reach quasi steady-state.

221

222 **3.3 Calibration approach**

223 We propose a calibration and validation approach involving three steps as illustrated in
224 Figure 2: (1) calibration of 1D models representing the flux measurement sites, (2) use of parameter
225 values from step 1 as initial values in the calibration of the distributed catchment model, and (3)
226 validation of the distributed parameterization on independent data. Additionally we test the
227 calibration results by comparing to model results based on 1D calibration only and with no
228 calibration respectively.

229 Both the 1D and the distributed simulations were calibrated using inverse modelling
230 adopting initial and range of parameter values from literature, observations, databases and
231 simulation results from the model code Daisy (Hansen et al. 1990, 1991) as described above and as
232 listed in Table 1 and 2. The initial input parameter values as well as their ranges were specified
233 according to relevance: If available, either observations or Daisy model simulations based on site
234 specific conditions were used. When using literature values conditions similar to the sites in terms
235 of vegetation species, climate and soil type were used. The calibration period covers a one year
236 period from October 1, 2009 to September 30, 2010 while the validation period is from May 1,
237 2011 to April 30, 2012.

238 The sensitivity and auto-calibration analyses were performed using the AUTOCAL software
239 included in the MIKE SHE package (Madsen 2003). At the point scale three components were
240 included in the objective function: latent heat flux LE, sensible heat flux H, and averaged soil water

241 content based on measurements at three depths (2.5, 22.5 and 52.5 cm below the surface). The
242 objective function was built from the root mean square errors (RMSE) between observations and
243 simulations. The RMSEs for the three individual components were normalized, weighted equally
244 and summed to arrive at an aggregated objective function. The normalization was carried out using
245 the common distance scale which has proven to be robust in accounting for differences in
246 magnitude of each component of the objective function (Madsen 2003, Butts et al. 2004, Mertens et
247 al. 2004).

248 At catchment scale the optimization was performed against two overall components of equal
249 weight: (1) Discharge observations at three discharge stations aggregated with equal weight (Figure
250 1) and (2) latent and sensible energy fluxes at the three sites weighted according to the relative areal
251 share of each land surface type (agriculture 62%, forest 13% and grass/meadow 25%).

252 The sensitivity analysis (Step 1.2 and 2.2 in Figure 2) for both point and catchment scales
253 were based on the AUTOCAL local sensitivity analysis procedure accounting for parameter
254 sensitivities at the location in parameter space defined by the initial parameter values. Since the
255 sensitivity analysis was local and therefore unable to account for numerous combinations in the
256 parameter space, the sensitivity analyses were repeated using randomly sampled parameter sets
257 within the parameter bounds. The sensitivity analysis was based on a backward difference
258 approximation method around the parameter value using a 2% perturbation fraction. Also,
259 covariance matrices were calculated to test for parameter correlation.

260 For both scales the ten most sensitive parameters were identified and subsequently used in
261 the auto-calibration process similar to Blasone et al. (2007). Only parameters with relative
262 sensitivity coefficients above 1%, in relation to the most sensitive parameter, were included in the
263 optimization (Hill 1998). For the low sensitivity parameters that were not included in the auto-

264 calibration of the catchment model their values were derived from the point scale calibrations. The
265 remaining distributed parameters were based on relevant literature (Table 2).

266 The point scale parameter optimization was based on the global Shuffled Complex
267 Evolution method (Duan et al. 1993) which has proven to be robust for comprehensive parameter
268 estimation problems (Butts et al. 2004, Mertens et al. 2005, Blasone et al. 2007). A maximum time
269 step of 6 minutes was used for the 1D models, which for the calibration period corresponded to a
270 computation time of around 2-3 minutes per model run. The model convergence criteria were
271 defined as max. 1% change in objective function after three iterations loops and this criterion was
272 usually met after 200-250 runs. For obtaining a more efficient optimization of the catchment scale
273 model, parallel model runs were carried out using the global Population Simplex Evolution
274 optimization method (DHI 2010). The convergence criterion was typically reached after 250-400
275 runs.

276 To assess the accuracy of the parameterization and modelling approach as such, an
277 independent validation analysis was performed subsequent to the auto-calibration simulations. The
278 validation was performed for a one-year period and assessed on discharge, LE and H as for the
279 calibration analysis (Step 3.1, Figure 2).

280

281 **3.4 Handling of Energy Balance Flux problems**

282 Energy balance closure requires that the net radiation (difference between incoming and
283 outgoing long- and short-wave radiation) equals the sum of latent heat (LE), sensible heat (H), and
284 soil heat (G) fluxes. All terms are highly sensitive to the surface characteristics and furthermore
285 they are subject to different diurnal and seasonal variations. The albedo of bare soil is dependent on
286 texture and moisture content while the albedo for vegetation generally decreases with vegetation
287 height and stand complexity. Changes in albedo will affect the amount of available energy, and soil

288 moisture influences how this energy is distributed between LE and H heat fluxes. Independent
289 measurements of the components of the energy balance equation rarely provide closure, which has
290 been documented in numerous studies (Wilson et al. 2002, Franssen et al. 2010, Leuning et al.
291 2012).

292 The impact of the energy balance closure problem on the calibration results was addressed
293 by creating four hypotheses each based on different assumptions regarding measurement errors
294 (Step 1.4 and 2.4, Figure 2). All four hypotheses were used for the 1D runs whereas only the first
295 two were used in the distributed runs to reduce computation time.

- 296 • HYP1: The measured energy fluxes (LE, H and G) are scaled with a single factor (increase)
297 such that the Bowen-ratio is maintained and the sum of the energy fluxes equals measured
298 net radiation over the one-year calibration period;
- 299 • HYP2: The measured energy fluxes are maintained whereas the net radiation is scaled with a
300 factor (reduction) to match the sum of measured energy fluxes over the one-year calibration
301 period;
- 302 • HYP3: The measured energy fluxes are unaltered whereas the sum of these is used as net
303 radiation on a daily basis;
- 304 • HYP4: The measured energy fluxes (LE, H and G) are scaled with a single factor (increase)
305 such that the Bowen-ratio is maintained and the sum of the energy fluxes equals measured
306 net radiation on a daily basis;

307 For the first two scenarios the entire dataset is multiplied by a single scaling factor to
308 provide energy closure for the one year calibration period. Closure on a daily basis may not be met,
309 which is the case for the last two scenarios. Of the investigated scenarios more energy is available
310 in HYP1 and HYP4 based on the measured net radiation (yearly mean values of 55 w/m^2 , 68 w/m^2

311 and 55 w/m² for agriculture, forest and meadow respectively) whereas HYP2 and HYP3 are based
312 on reduced values (yearly mean values of 39 w/m², 48 w/m² and 42 w/m² for the same sites).

313 Only the HYP1 and HYP2 hypotheses were used for the distributed simulations since they
314 both utilize measured net radiation, scaled and unscaled, and hereby the daily temporal pattern is
315 likely to be more representative than if based on the sum of the three fluxes. In contrast to the point
316 scale where net radiation measurements were available, global radiation was used in the catchment
317 scale analysis. To fulfil the same assumptions on energy balance closure as used at point scale the
318 albedo was adjusted to obtain energy balance closure over the entire one year calibration period.
319 This was done based on the flux measurements for the three general land use types agriculture,
320 forest and meadow. As a result HYP1 is based on measured albedos whereas HYP2 is based on
321 estimated albedos that are higher than measured. All three distributed simulation cases shown in
322 Figure 2 were performed for both HYP1 and HYP2 as well as for the calibration and validation
323 periods for a total of 12 simulations.

324

325 **4 Results**

326 **4.1 Energy balance closure**

327 The measurements used in this study show lack of energy balance closure. The sum of LE,
328 H and G over the one-year calibration period accounted for 71%, 71% and 76% of the measured net
329 radiation at the agricultural, forest and meadow/grass sites respectively (Figure 3). The
330 corresponding measured Bowen-ratios in the same period were 0.20, 0.17 and 0.18 for the three
331 land surface types. Radiation and particularly data for energy fluxes are generally sparse in
332 Denmark. Therefore, in Figure 3, measured net and global radiation as well as the sum of energy
333 fluxes are compared to results from (1) the corresponding grid cell in HIRHAM regional climate
334 model simulations (Larsen et al. 2013) using ERA-Interim reanalysis data as boundary conditions

335 and (2) observation data from the Foulum research station (grass surface) located app. 50 km north
336 of the agriculture and forest sites. HIRHAM simulation data are also used to compare LE and H
337 fluxes since no other flux data were available. The simulations of net radiation by HIRHAM and the
338 observed data from Foulum are much closer to measured LE, H and G flux sum at all sites for both
339 years although perhaps less distinct at the forest site (Figure 3). For global radiation there is a close
340 match between all data series, especially between the three study sites and Foulum. For LE fluxes
341 good agreement is seen between HIRHAM simulations and observations for the forest and meadow
342 sites and less favourable for the agricultural site. For the H fluxes larger discrepancies are seen
343 particularly for the forest site.

344

345 4.2 Simulation results

346 The results of the sensitivity analyses for both point and catchment scales are shown in
347 Figure 4. Similar parameter sensitivity results are obtained for the agricultural and forest sites with
348 nine and ten parameters, respectively, having a relative sensitivity coefficient above 10%. The
349 parameter sensitivities for hypotheses HYP2 and HYP3 (with unaltered energy fluxes) show similar
350 patterns with the minimal stomata resistance (R_{st_min}) as the most sensitive parameter. In contrast,
351 for hypotheses HYP1 and HYP4 (with corrected energy fluxes) the root shape factor is the most
352 sensitive parameter. For the meadow site only the three parameters R_{st_min} , leaf area index (LAI)
353 and vegetation height have relative sensitivity coefficients above 10% and the influence of the
354 energy balance hypothesis is limited given the large drop in sensitivity between R_{st_min} and the
355 second most sensitive parameter LAI.

356 At catchment scale saturated hydraulic conductivity (K_{sat}) for the unsaturated zone is the
357 most sensitive parameter for both energy balance hypotheses, whereas the sensitivities of the
358 remaining parameters are smaller and also subject to larger variation between the two hypotheses

359 (Figure 4). The forest energy fluxes were found to be poorly reproduced by the calibrated forest leaf
360 width values which were therefore manually calibrated prior to auto-calibration.

361 The simulated discharge based on the parameter values obtained by the full auto-calibration
362 approach for the two distributed energy balance hypotheses are shown in Figure 5 for both the
363 calibration and validation periods. For both simulations and periods there is a tendency of
364 underestimation of baseflow and mostly pronounced for HYP2. For peak flow the HYP2 hypothesis
365 exhibits more dynamic behaviour with more rapid responses. In summary, the HYP1 simulation
366 shows better discharge performance statistics for the calibration period whereas the opposite pattern
367 is seen for the validation period (Figure 6). Also, the validation confirms a reasonable discharge
368 calibration although the HYP1 results are moderately poorer for two out of three discharge stations.

369 Figure 7 shows simulated LE and H energy fluxes on an hourly basis for a 10 day summer
370 period in the calibration period. The results from the two energy hypothesis runs are compared to
371 their relevant fluxes: HYP1 to scaled and HYP2 to unscaled fluxes, corresponding to the
372 assumptions of the energy balance closure. For both the calibration and validation periods, there is a
373 tendency for better energy flux statistics for HYP2 compared to HYP1 (Figure 6). Overall the
374 agriculture and grass surfaces are better reproduced compared to forest. Especially observations of
375 H in the forest are rather poorly simulated during high global radiation (Figure 7); however, part of
376 this discrepancy is likely caused by errors in the observation data (Sonnenborg et al. 2013).
377 Simulations for night time conditions compare favourably to observations of both energy fluxes and
378 for both scenarios. As shown in Figure 6 the simulations for the validation period shows
379 comparable or better performance statistics for both fluxes as compared to the calibration period.

380 In the auto-calibration, simulations are compared to the same observed discharge data for
381 both HYP1 and HYP2 while the energy fluxes and albedos were adjusted to obtain energy balance
382 closure. This is reflected by differences in water balance components for the two hypotheses HYP1

383 and HYP2 both on catchment and local scales (Table 3). With a lower albedo in the HYP1 scenario
384 higher ET and therefore lower recharge and discharge are simulated at catchment scale. For the
385 agriculture grid cell the slightly higher ET for the HYP2 hypothesis can be ascribed to the lower
386 K_{sat} value. The significant difference in drainage is likely a function of higher groundwater
387 elevations in the HYP2 hypothesis. For forest and meadow the difference in albedo is reflected in
388 higher ET for HYP1.

389 The comparison of the performances of the full calibration and the scenarios with calibration
390 of the 1D models only and no calibration respectively is shown in figure 6. For discharge the
391 simulations with no calibration using default values is comparable to the results of the full
392 calibration whereas the 1D calibration is generally poorer. The most significant improvement in the
393 calibration approach is however seen for the LE and H energy fluxes where the mean root mean
394 square error (RMSE) and mean absolute error (MAE) statistics for the three sites is substantially
395 improved. The distributed simulations based on the values from the 1D calibration transferred to
396 catchment scale are generally of lower quality compared to the case where no calibration is carried
397 out. This, as opposed to using initial values using no calibration at all (default values), is because
398 neither input source includes parameters related to the distributed scale (e.g. related to discharge
399 and overland flow). Also, the extreme 1D mean RMSE statistics for H is due to the forest site which
400 was manually calibrated prior to the autocalibration (see above) and it does therefore not affect the
401 full 1D+2D calibration.

402

403 **5 Discussion**

404 We have presented an approach for a stepwise calibration of a distributed combined land
405 surface/hydrology model using observations of energy fluxes and discharge as calibration target. In
406 general the method proved effective. The validation period confirmed the performance statistics

407 from the calibration period and the simulations using a reduced calibration approach or no
408 calibration were generally less accurate.

409

410 **5.1 Energy and water balance**

411 As expected a key finding was that the choice of energy balance hypothesis has a major
412 impact on the resulting parameterization as well as on the energy and water balance results. The
413 lack of energy balance closure for flux measurements is therefore a great challenge when using such
414 measurements for calibrating distributed hydrological models. Energy balance closure is required
415 when flux measurements are used for inverse modelling and we investigated two hypotheses where
416 the error was attributed to either the measured energy fluxes (HYP1) or the measured net radiation
417 (HYP2).

418 Either of these two approaches may be applicable. Even though the eddy covariance method
419 is generally regarded as the best practical method for measuring energy fluxes, measurement
420 difficulties are well documented (Foken et al. 2006, Sun et al. 2008, Franssen et al. 2010, Ringgard,
421 2012, Stoy et al. 2013). A consistent deficit in measured LE fluxes have been suggested as an
422 explanation in the lack of energy balance closure (Sun et al. 2008) while on the other hand Foken et
423 al. (2006) suggested that low frequency turbulence structures cause errors in the flux measurements.
424 Also, measurement errors in H fluxes have been suggested, see (Mauder et al. 2008) and
425 Sonnenborg et al. (2013). The energy flux statistics (Figure 6) were better for the HYP2 hypothesis
426 possibly indicating that larger measurement errors are attributed to the energy fluxes compared to
427 radiation components. An additional contributing factor is the difference in the footprint of the flux
428 measurements reflecting conditions upstream of the wind direction and the support scale of the
429 radiation sensor.

430 Contrary to indications of flux measurement biases, estimates of ET based on eddy
431 covariance and soil moisture balances of the root zone compared well and surprisingly the highest
432 ET was seen for the eddy covariance method over a seven week period in May-June 2009 (Schelde
433 et al. 2011). Similarly, net radiation measurements from Foulum research station match the sum of
434 LE, H and G fluxes better than for the agriculture, forest and meadow sites used in this study
435 (Figure 3). Advection has also been suggested as a missing component in the energy balance
436 suggesting that the measured energy fluxes may indeed be more reliable than anticipated (Leuning
437 et al. 2012). Likewise, large scale eddies due to land surface heterogeneity have recently been
438 suggested to make up a part of the energy imbalance (Stoy et al. 2013).

439 Snow processes are currently not considered the SWET land-surface model and this impacts
440 the calibration results especially with regard to discharge. Even though the calibration period is
441 relatively cold, little precipitation occurs on days with temperatures below 0 °C. Nevertheless, the
442 snow melt related discharge peaks in Feb-Mar 2010 are clearly not reproduced (Figure 5).

443

444 **5.2 Sensitivity, calibration and validation**

445 The distinct differences between parameter sensitivities at the agriculture and forest sites
446 compared to the meadow site are related to the water available for ET (Figure 8). At the agricultural
447 and forest sites, complete soil saturation is rarely or never reached and there is a clear tendency for
448 higher ET with lower soil moisture as this occurs during the summer months with a higher level of
449 available solar energy. Soil parameters affecting available soil water are therefore crucial for
450 determining the partitioning of energy fluxes at these sites. For the meadow site, located next to the
451 river bank, saturated conditions are often reached (41% of the year for HYP2) and soil moisture
452 levels are generally high. As a result the relation between root zone water and ET is less distinct.

453 The high water availability at the meadow site therefore makes vegetation parameters substantially
454 more important compared to soil parameters.

455 The choice of energy balance closure hypothesis, and therefore the energy available, is
456 highly influential on which parameters are most sensitive especially for the agriculture and forest
457 sites but also to some extent for the meadow site. This is reflected in the sensitivities for the HYP1
458 and HYP4 hypotheses on one side and the HYP2 and HYP3 hypotheses on the other. This is
459 consistent with the HYP1/HYP4 hypotheses being based on measured net radiation (averaged to 54,
460 67 and 56 W/m^2 in the calibration period for agriculture, forest and meadow) while the
461 HYP2/HYP3 hypotheses are based on downscaled net radiation (40, 47 and 40 W/m^2 for the same
462 sites).

463 The results of the sensitivity analysis and auto-calibration procedure naturally reflect the
464 interplay between a vast number of parameters, assumptions regarding the energy balance terms,
465 assumed relations between parameters for the individual soil layers, and the specific conditions that
466 apply for the period subject to the analysis. These assumptions are required for reasons such as
467 energy balance closure, calibration simplicity, data availability and focus of the study in question.
468 For example, the parameter R_{st_min} is assumed constant in the present study whereas Ingwersen et
469 al. (2011) obtained better simulations of LE and H based on the Noah LSM model using monthly
470 values of R_{st_min} . Hou et al. (2012) related simulations of LE and H to parameter uncertainty in a
471 study using the Community Land Model (CLM4) and documented substantial variations in the
472 simulations of both fluxes (over 100 W/m^2) in the summer months depending on the
473 parameterization. The rather poor agreement between simulations and observations of H fluxes was
474 likely due to observation errors. Separate auto-calibration runs were performed assessing forest heat
475 fluxes based on forest parameterization alone with limited improvement and this is in line with the
476 results by Sonnenborg et al. (2013).

477

478 **5.3 Land use**

479 Standard seasonal crop characteristics were used in this study and the actual crop rotation
480 and management conditions at a given site were therefor not considered. This could lead to
481 discrepancies between the vegetation parameterization at the agricultural site particular around the
482 time of harvest and at the grass site due to irregular and undocumented cattle grazing. Possibly
483 more significant is the effect of the spatial distribution of crops derived from available county
484 average data, which may not reflect the actual distribution. This is the case both in terms of the
485 overall distribution, type and location of crops within the catchment. But it also affects the
486 evaluation of energy flux data from the agricultural site as the actual footprint may differ from the
487 simulated crop as also reported by Göckede et al. (2008).

488 The distributed MIKE SHE parameterization was performed by transferring the calibrated
489 parameters from the point scale setups, representing agriculture, meadow and forest, to the relevant
490 land surfaces within the catchment for subsequent sensitivity and auto-calibration analyses. For
491 agriculture, this procedure includes the tradeoff between using the calibrated parameter values
492 reflecting site specific conditions at the measurement site and using crop and soil specific
493 parameters from the Daisy model. However, the former was used since parameters were calibrated
494 under conditions of energy balance closure but also because of the statistical spatial distribution of
495 the Daisy modelled crop characteristics.

496

497 **6 – Conclusions**

498 In the present study we present a novel approach to calibrating a combined and distributed
499 hydrology/land-surface model. The approach first involves calibration of the land-surface model
500 component against measurements of energy fluxes from flux towers. Secondly, the distributed

501 hydrological model component, including unsaturated and saturated zone components, is calibrated
502 using the point scale parameterization as initial conditions and using stream flow and energy flux
503 measurements as the calibration targets. The method employs a meticulous literature inspection for
504 realistic initial and range of parameter values. Previous calibration efforts of SVAT and LSM
505 models with a hydrological focus have often used satellite data having certain measurement
506 deficiencies, relied on previously point scale based parameterizations or used traditional
507 hydrological variables such as discharge and hydraulic head. Modelling the highly interrelated and
508 dynamical processes and variables in the entire water and energy budget from groundwater to lower
509 atmosphere is challenging. Our results show that the proposed approach significantly improves the
510 simulated energy balance components as compared to using default values or a simpler 1D
511 calibration. The simulations were able to reproduce features across water and energy budgets taking
512 into considerations measurement errors and lack of energy balance closure.

513 The calibration of the one dimensional models provided good insight to data quality and
514 parameter sensitivity and served as a useful initial parameterization of the catchment scale
515 simulations. Further, the sensitivities of parameters in the point scale analysis were highly affected
516 by the surface type and more specifically the water availability as well as the choice of energy
517 balance hypothesis. Similarly, the catchment model simulations showed that parameter sensitivities
518 are largely determined by the choice of energy balance hypothesis, yet saturated hydraulic
519 conductivity was the most sensitive parameter for both energy balance hypotheses. Despite likely
520 errors in measured forest sensible heat fluxes, our results suggest that the measured energy fluxes
521 are reliable and that the energy imbalance is likely caused by advection and large scale eddies rather
522 than erroneous net radiation measurements.

523

524 **7 - Acknowledgments**

525 The present study was funded by a grant from the Danish Strategic Research Council for the project
 526 HYdrological Modelling for Assessing Climate Change Impacts at differeNT Scales (HYACINTS–
 527 www.hyacints.dk) under contract no: DSF-EnMi 2104-07-0008. The study is made possible
 528 through a collaboration with the HOBE project (www.hobecenter.dk) funded by the Villum Kann
 529 Rasmussen Foundation. The data used in the study can be accessed through the first author.

530

531

532

533

534 8 – References

- 535 • Allerup, P., Madsen, H., Vejen, F., 1998. Standardværdier (1961-90) af Nedbørkorrektioner, Danish
 536 Meteorological Institute Technical Report 98-10, Denmark.
- 537 • [Barr, A.G., van der Kamp, G., Black, T.A., McCaughey, J.H., Nesic, Z., 2012. Energy balance closure at](#)
 538 [the BERMS flux towers in relation to the water balance of the White Gull Creek watershed 1999–2009.](#)
 539 [Agric. Forest Meteorol. 153, 3–13. doi:10.1016/j.agrformet.2011.05.017.](#)
- 540 • Beier, C., Gundersen, P., Hansen, K., Rasmussen, L., 1995. Experimental manipulation of water and
 541 nutrient input to a Norway spruce plantation at Klosterhede, Denmark. Plant Soil 168, 613–622.
- 542 • Beven, K.J., Franks, S.W., 2001. Functional similarity in landscape scale SVAT modelling. Hydrol.
 543 Earth Syst. Sc. 3, 85–93. doi:10.5194/hess-3-85-1999
- 544 • Beven, K., 2006. Searching for the Holy Grail of scientific hydrology: $Q_t = (S, R, ?_t) A$ as closure.
 545 Hydrol. Earth Syst. Sc. Discussions 10, 609–618. doi:10.5194/hess-10-609-2006.
- 546 • Blasone, R. S., Madsen, H., Rosbjerg, D., 2007. Parameter estimation in distributed hydrological
 547 modelling: comparison of global and local optimisation techniques, Nord. Hydrol. 38(4–5), 451–476,
 548 doi:10.2166/nh.2007.024.
- 549 • Boulet, G., Kalma, J.D., Braud, I., Vauclin, M., 1999. An assessment of effective land surface
 550 parameterisation in regional-scale water balance studies. J. Hydrol. 217, 225–238.

- 551 • Breda, N.J.J., 2003. Ground-based measurements of leaf area index: a review of methods, instruments
552 and current controversies. *J. Exp. Bot.* 54, 2403–2417. doi:10.1093/jxb/erg263
- 553 • Butts, M. B., Payne, J. T., Kristensen, M., Madsen, H., 2004. An evaluation of the impact of model
554 structure on hydrological modelling uncertainty for streamflow simulation, *J. Hydrol.* 298, 242–266,
555 doi:10.1016/j.jhydrol.2004.03.042.
- 556 • Butts, M., Drews, M., Larsen, M.A.D., Lerer, S., Rasmussen, S.H., Grooss, J., Overgaard, J., Refsgaard,
557 J.C., Christensen, O.B., Christensen, J.H., 2014. Embedding complex hydrology in the regional climate
558 system – Dynamic coupling across different modelling domains. *Adv. Water Resour.* 74, 166–184.
559 doi:10.1016/j.advwatres.2014.09.004
- 560 • Boegh, E., Poulsen, R.N., Butts, M., Abrahamsen, P., Dellwik, E., Hansen, S., Hasager, C.B., Ibrom, A.,
561 Loerup, J.-K., Pilegaard, K., Soegaard, H., 2009. Remote sensing based evapotranspiration and runoff
562 modeling of agricultural, forest and urban flux sites in Denmark: From field to macro-scale. *J. Hydrol.*
563 377, 300–316. doi:10.1016/j.jhydrol.2009.08.029
- 564 • Chen, F., Dudhia, J., 2001a. Coupling an Advanced Land Surface–Hydrology Model with the Penn
565 State–NCAR MM5 Modeling System. Part I: Model Implementation and Sensitivity. *Mon. Wea. Rev.*
566 129, 569–585. doi:10.1175/1520-0493(2001)129<0569:CAALSH>2.0.CO;2
- 567 • Choi, M., Kustas, W.P., Anderson, M.C., Allen, R.G., Li, F., Kjaersgaard, J.H., 2009. An
568 intercomparison of three remote sensing-based surface energy balance algorithms over a corn and
569 soybean production region (Iowa, U.S.) during SMACEX. *Agric. For. Meteorol.* 149, 2082–2097.
570 doi:10.1016/j.agrformet.2009.07.002
- 571 • Crow, P., 2005. The Influence of Soils and Species on Tree Root Depth, Environmental and Human
572 Sciences Division, Forest Research. ISBN 0-85538-679-7, United Kingdom.
- 573 • Dai, Z., Li, C., Trettin, C., Sun, G., Amatya, D., Li, H., 2010. Bi-criteria evaluation of the MIKE SHE
574 model for a forested watershed on the South Carolina coastal plain. *Hydrol. Earth Syst. Sc.* 14, 1033–
575 1046. doi:10.5194/hess-14-1033-2010.

- 576 • Demarty, J., Otlé, C., Braud, I., Olivos, A., Frangi, J., Bastidas, L., Gupta, H., 2004. Using a
577 multiobjective approach to retrieve information on surface properties used in a SVAT model. *J. Hydrol.*
578 287, 214–236. doi:10.1016/j.jhydrol.2003.10.003
- 579 • DHI, 2010. AUTOCAL – Auto Calibration Tool, User Guide. MIKE by DHI Software, Hørsholm,
580 Denmark.
- 581 • Duan, Q., Gupta, V. K., Sorooshian, S., 1993. A shuffled complex evolution approach for effective and
582 efficient global minimization, *J Optimiz. Theory. Ap.*, 76, 501-521.
- 583 • Ewers, B.E., Oren, R., Johnsen, K.H., Landsberg, J.J., 2001. Estimating maximum mean canopy stomatal
584 conductance for use in models. *Can. J. Forest Res.* 31, 198–207. doi:10.1139/cjfr-31-2-198
- 585 • Foken T, Wimmer, F., Mauder, M., Thomas, C., Liebethal, C., 2006. Some aspects of the energy balance
586 closure problem, *Atmos. Chem. Phys.*, 6, 3381–3402, doi:10.5194/acp-6-4395-2006.
- 587 • Frank, A.B., Bittman, S., Johnson, D.A., 1996. Water relations of cool-season grasses. Cool-season
588 forage grasses, L.E. Moser et al. (ed.), *Agron. Monogr.*, 34, 127-164, ASA, CSSA, SSSA, Madison,
589 Wisconsin, USA.
- 590 • Franks, S.W., Beven, K.J., Quinn, P.F., Wright, I.R., 1997. On the sensitivity of soil-vegetation-
591 atmosphere transfer (SVAT) schemes: equifinality and the problem of robust calibration. *Agric. For.*
592 *Meteorol.* 86, 63–75. doi:10.1016/S0168-1923(96)02421-5
- 593 • Franks, S.W., Beven, K.J., Gash, J.H.C., 1999. Multi-objective conditioning of a simple SVAT model.
594 *Hydrol. Earth Syst. Sc. Discussions* 3, 477–488.
- 595 • Franssen, H.J.H., Stöckli, R., Lehner, I., Rotenberg, E., Seneviratne, S.I., 2010. Energy balance closure
596 of eddy-covariance data: A multisite analysis for European FLUXNET stations. *Agric. For. Meteorol.*
597 150, 1553–1567. doi:10.1016/j.agrformet.2010.08.005
- 598 • Graham, D. N., Butts, M.B., 2005. Flexible, integrated watershed modelling with MIKE SHE, In
599 *Watershed Models*, Eds. V.P. Singh & D.K. Frevert, 245-272, CRC Press. ISBN: 0849336090.

- 600 • Greve, M.H., Greve, M.B., Bøcher, P.K., Balstrøm, T., Breuning-Madsen, H., Krogh, L., 2007.
 601 Generating a Danish raster-based topsoil property map combining choropleth maps and point
 602 information. *Geografisk Tidsskrift-Danish Journal of Geography* 107, 1–12.
- 603 • Gryning, S.-E., Batchvarova, E., De Bruin, H.A.R., 2001. Energy balance of a sparse coniferous high-
 604 latitude forest under winter conditions. *Bound.-Layer Meteor.* 99, 465–488.
- 605 • Göckede, M., Foken, T., Aubinet, M., Aurela, M., Banza, J., Bernhofer, C., Bonnefond, J.M., Brunet, Y.,
 606 Carrara, A., Clement, R., Dellwik, E., Elbers, J., Eugster, W., Fuhrer, J., Granier, A., Grünwald, T.,
 607 Heinesch, B., Janssens, I.A., Knohl, A., Koeble, R., Laurila, T., Longdoz, B., Manca, G., Marek, M.,
 608 Markkanen, T., Mateus, J., Matteucci, G., Mauder, M., Migliavacca, M., Minerbi, S., Moncrieff, J.,
 609 Montagnani, L., Moors, E., Ourcival, J.-M., Papale, D., Pereira, J., Pilegaard, K., Pita, G., Rambal, S.,
 610 Rebmann, C., Rodrigues, A., Rotenberg, E., Sanz, M.J., Sedlak, P., Seufert, G., Siebicke, L., Soussana,
 611 J.F., Valentini, R., Vesala, T., Verbeeck, H., Yakir, D., 2008. Quality control of CarboEurope flux data –
 612 Part 1: Coupling footprint analyses with flux data quality assessment to evaluate sites in forest
 613 ecosystems. *Biogeosciences* 5, 433–450. doi:10.5194/bg-5-433-2008
- 614 • Grimmond, C.S.B., Blackett, M., Best, M.J., Barlow, J., Baik, J.-J., Belcher, S.E., Bohnenstengel, S.I.,
 615 Calmet, I., Chen, F., Dandou, A., Fortuniak, K., Gouvea, M.L., Hamdi, R., Hendry, M., Kawai, T.,
 616 Kawamoto, Y., Kondo, H., Krayenhoff, E.S., Lee, S.-H., Loridan, T., Martilli, A., Masson, V., Miao, S.,
 617 Oleson, K., Pigeon, G., Porson, A., Ryu, Y.-H., Salamanca, F., Shashua-Bar, L., Steeneveld, G.-J.,
 618 Tombrou, M., Voogt, J., Young, D., Zhang, N., 2010. The International Urban Energy Balance Models
 619 Comparison Project: First Results from Phase 1. *J. Appl. Meteorol.* 49, 1268–1292.
 620 doi:10.1175/2010JAMC2354.1
- 621 • Gupta, H.V., Sorooshian, S., Yapo, P.O., 1998. Toward improved calibration of hydrologic models:
 622 Multiple and noncommensurable measures of information. *Water Resour. Res.* 34, 751–763.
 623 doi:10.1029/97WR03495
- 624 • Gupta, H.V., Bastidas, L.A., Sorooshian, S., Shuttleworth, W.J., Yang, Z.L., 1999. Parameter estimation
 625 of a land surface scheme using multicriteria methods. *J. Geophys. Res.* (1984–2012) 104, 19491–19503.

- 626 • Hansen, S., Jensen, H. E., Nielsen, N. E., Svendsen H., 1990. Daisy: Soil-plant-atmosphere system
627 model. NPO National Agency of Environmental Protection Research Report No. A10. Copenhagen,
628 Denmark.
- 629 • Hansen, S., Jensen, H. E., Nielsen, N. E., Svendsen H., 1991. Simulation of nitrogen dynamics and
630 biomass production in winter wheat using the Danish simulation model DAISY. *Fert. Res.*, 27, 245-259.
- 631 • Hassan, Q.K., Bourque, C.P.-A., 2010. Spatial Enhancement of MODIS-based Images of Leaf Area
632 Index: Application to the Boreal Forest Region of Northern Alberta, Canada. *Remote Sens.* 2, 278–289.
633 doi:10.3390/rs2010278
- 634 • Hill, M.C., 1998. Methods and Guidelines for Effective Model Calibration. U.S. Geological Survey
635 Water-Resources Investigations Report 98-4005, USA.
- 636 • Hou, Z., Huang, M., Leung, L. R., Lin, G., Ricciuto, D. M., 2012. Sensitivity of surface flux simulations
637 to hydrologic parameters based on an uncertainty quantification framework applied to the Community
638 Land Model, *J. Geophys. Res.*, 117, D15108, doi:10.1029/2012JD017521.
- 639 • Hussein, A.S., 1999. Grass ET estimates using Penman-type equations in Central Sudan. *J. Irrig. Drain.*
640 *Eng.* 125, 324–329.
- 641 • Højberg, A. L., Trolborg, L., Stisen, S., Christensen, B. B. S., Henriksen, H. J., 2013. Stakeholder
642 driven update and improvement of a national water resources model, *Environ. Modell. Softw.*, 40, 202-
643 213. doi:10.1016/j.envsoft.2012.09.010
- 644 • Ingwersen, J., Steffens, K., Högy, P., Warrach-Sagi, K., Zhunusbayeva, D., Poltoradnev, M., Gäbler, R.,
645 Witzmann, H.-D., Fangmeier, A., Wulfmeyer, V., Streck, T., 2011. Comparison of Noah simulations with
646 eddy covariance and soil water measurements at a winter wheat stand. *Agric. For. Meteorol.* 151, 345–
647 355. doi:10.1016/j.agrformet.2010.11.010
- 648 • Iversen, B. V., Børgesen, C. D., Lægdsmand, M., Greve, M. H., Heckrath, G., Kjærgaard, C., 2011. Risk
649 Predicting of Macropore Flow using Pedotransfer Functions, Textural Maps, and Modeling. *Vadose Zone*
650 *J.*, 10, 1185–1195, doi:10.2136/vzj2010.0140.

- 651 • Jensen, K.H., Illangasekare, T. H., 2011. HOBE: A Hydrological Observatory. *Vadoze Zone J.* 10, 1-7,
652 doi:10.2136/vzj2011.0006.
- 653 • Kelliher, F.M., Leuning, R., Raupach, M.R., Schulze, E.-D., 1995. Maximum conductances for
654 evaporation from global vegetation types. *Agr. Forest. Meteorol.* 73, 1–16. doi:10.1016/0168-
655 1923(94)02178-M
- 656 • Lagergren, F., Eklundh, L., Grelle, A., Lundblad, M., Mölder, M., Lankreijer, H., Lindroth, A., 2005. Net
657 primary production and light use efficiency in a mixed coniferous forest in Sweden. *Plant, Cell &*
658 *Environ.* 28, 412–423. doi:10.1111/j.1365-3040.2004.01280.x
- 659 • Lantinga, E.A., Nassiri, M., Kropff, M.J., 1999. Modelling and measuring vertical light absorption
660 within grass–clover mixtures. *Agr. Forest. Meteorol.* 96, 71–83.
- 661 • Larsen, M. A. D., Thejll, P., Christensen, J. H., Refsgaard, J. C., Jensen, K. H., 2013. On the role of
662 domain size and resolution in the simulations with the HIRHAM region climate model, *Clim Dyn* 40,
663 2903–2918, doi:10.1007/s00382-012-1513-y.
- 664 • Larsen, M.A.D., Refsgaard, J.C., Drews, M., Butts, M.B., Jensen, K.H., Christensen, J.H., Christensen,
665 O.B., 2014. Results from a full coupling of the HIRHAM regional climate model and the MIKE SHE
666 hydrological model for a Danish catchment. *Hydrol. Earth. Syst. Sc.* 18, 4733–4749. doi:10.5194/hess-
667 18-4733-2014
- 668 • Lawrence, D.M., Oleson, K.W., Flanner, M.G., Thornton, P.E., Swenson, S.C., Lawrence, P.J., Zeng, X.,
669 Yang, Z.-L., Levis, S., Sakaguchi, K., Bonan, G.B., Slater, A.G., 2011. Parameterization improvements
670 and functional and structural advances in Version 4 of the Community Land Model. *J. Adv. Model. Earth*
671 *Syst.* 3, M03001. doi:10.1029/2011MS00045
- 672 • Lazzarotto, P., Calanca, P., Fuhrer, J., 2009. Dynamics of grass–clover mixtures—An analysis of the
673 response to management with the PROductive GRASSland Simulator (PROGRASS). *Ecol. Model.* 220,
674 703–724. doi:10.1016/j.ecolmodel.2008.11.023
- 675 • Lazzarotto, P., Calanca, P., Semenov, M., Fuhrer, J., 2010. Transient responses to increasing CO₂ and
676 climate change in an unfertilized grass–clover sward. *Clim. Res.* 41, 221–232. doi:10.3354/cr00847

- 677 • Leuning, R., van Gorsel, E., Massman, W.J., Isaac, P.R., 2012. Reflections on the surface energy
678 imbalance problem. *Agric. For. Meteorol.* 156, 65–74. doi:10.1016/j.agrformet.2011.12.002
- 679 • Li, H., Huang, M., Wigmosta, M.S., Ke, Y., Coleman, A.M., Leung, L.R., Wang, A., Ricciuto, D.M.,
680 2011. Evaluating runoff simulations from the Community Land Model 4.0 using observations from flux
681 towers and a mountainous watershed. *J. Geophys. Res.* 116, (D24120). doi:10.1029/2011JD016276
- 682 • Lindroth, A., Lagergren, F., Aurela, M., Bjarnadottir, B., Christensen, T., Dellwik, E., Grelle, A., Ibrom,
683 A., Johansson, T., Lankreijer, H., Launiainen, S., Laurila, T., MöLder, M., Nikinmaa, E., Pilegaard, K.,
684 Sigurdsson, B.D., Vesala, T., 2008. Leaf area index is the principal scaling parameter for both gross
685 photosynthesis and ecosystem respiration of Northern deciduous and coniferous forests. *Tellus B* 60,
686 129–142. doi:10.1111/j.1600-0889.2007.00330.x
- 687 • Madsen, H., 2003. Parameter estimation in distributed hydrological catchment modelling using
688 automatic calibration with multiple objectives. *Adv. Water Resour.* 26, 205–216.
- 689 • Mauder, M., Desjardins, R. L., Pattey, E., Gao, Z., van Haarlem, R., 2008. Measurement of the Sensible
690 Eddy Heat Flux Based on Spatial Averaging of Continuous Ground-Based Observations. *Bound.-Layer*
691 *Meteorol.* 128, 151–172. doi:10.1007/s10546-008-9279-9
- 692 • Maurer, E.P., Wood, A.W., Adam, J.C., Lettenmaier, D.P., Nijssen, B., 2002. A long-term hydrologically
693 based dataset of land surface fluxes and states for the conterminous United States. *J. Climate* 15, 3237–
694 3251.
- 695 • Mauser, W., Schädlich, S., 1998. Modelling the spatial distribution of evapotranspiration on different
696 scales using remote sensing data. *J. Hydrol.* 212, 250–267.
- 697 • Maxwell, R.M., Lundquist, J.K., Mirocha, J.D., Smith, S.G., Woodward, C.S., Tompson, A.F.B., 2011.
698 Development of a Coupled Groundwater–Atmosphere Model. *Mon. Weather Rev.* 139, 96–116.
699 doi:10.1175/2010MWR3392.1
- 700 • Mertens, J., Madsen, H., Feyen, L., Jacques, D., Feyen, J., 2004. Including prior information in the
701 estimation of effective soil parameters in unsaturated zone modelling. *J. Hydrol.*, 294, 251–269,
702 doi:10.1016/j.jhydrol.2004.02.011.

- 703 • Mertens, J., Madsen, H., Kristensen, M., Jacques, D., Feyen, J., 2005. Sensitivity of soil parameters in
 704 unsaturated zone modelling and the relation between effective, laboratory and in situ estimates, *Hydrol.*
 705 *Process.*, 19, 1611–1633, doi:10.1002/hyp.5591.
- 706 • Meyer, P. D., Rockhold, M. L., Wee, G. W., 1997. Uncertainty analyses of infiltration and subsurface
 707 flow and transport for SDMP sites. Division of Regulatory Applications Office of Nuclear Regulatory
 708 Research, U.S. Nuclear Regulatory Commission, Washington, USA.
- 709 • Moore, C., Doherty, J., 2005. Role of the calibration process in reducing model predictive error. *Water*
 710 *Resour. Res.* 41, W05020. doi:10.1029/2004WR003501
- 711 • Nghi, V. V., Dung, D. D., Lam, D. T., 2008. Potential evapotranspiration estimation and its effect on
 712 hydrological model response at the Nong Son Basin, *VNU Journal of Science, Earth Sciences*, 24, 213-
 713 223.
- 714 • Olesen, J.E., Berntsen, J., Hansen, E.M., Petersen, B.M., Petersen, J., 2002. Crop nitrogen demand and
 715 canopy area expansion in winter wheat during vegetative growth. *Eur. J. Agron.* 16, 279–294.
 716 doi:10.1016/S1161-0301(01)00134-4
- 717 • Olesen, J.E., Hansen, P.K., Berntsen, J., Christensen, S., 2004. Simulation of above-ground suppression
 718 of competing species and competition tolerance in winter wheat varieties. *Field Crop. Res.* 89, 263–280.
 719 doi:10.1016/j.fcr.2004.02.005
- 720 • Overgaard, J., 2005. Energy-based land-surface modelling: new opportunities in integrated hydrological
 721 modeling, Ph.D. Thesis, Institute of Environment and Resources, DTU, Technical University of
 722 Denmark.
- 723 • Perry, D. A., 1994. *Forest Ecosystems*. The Johns Hopkins University Press, Maryland. 1. Ed. ISBN 0-
 724 8018-4760-5.
- 725 • Pollacco, J.A.P., Mohanty, B.P., Efstratiadis, A., 2013. Weighted objective function selector algorithm for
 726 parameter estimation of SVAT models with remote sensing data: Parameter Estimation for Svat Model.
 727 *Water Resour. Res.* 49, 6959–6978. doi:10.1002/wrcr.20554

- 728 • Pokorný, R., Tomášková, I., Havráňková, K., 2008. Temporal variation and efficiency of leaf area index
729 in young mountain Norway spruce stand. *Eur. J. For. Res.* 127, 359–367. doi:10.1007/s10342-008-0212-
730 z
- 731 • Rautiainen, M., Heiskanen, J., Korhonen, L., 2012. Seasonal changes in canopy leaf area index and
732 MODIS vegetation products for a boreal forest site in central Finland, *Boreal Environ. Res.*, 17, 72-84.
- 733 • Ridler, M.E., Sandholt, I., Butts, M., Lerer, S., Mougin, E., Timouk, F., Kergoat, L., Madsen, H., 2012.
734 Calibrating a soil–vegetation–atmosphere transfer model with remote sensing estimates of surface
735 temperature and soil surface moisture in a semi arid environment. *J. Hydrol.* 436-437, 1–12.
736 doi:10.1016/j.jhydrol.2012.01.047
- 737 • Ringgaard, R., 2012. On variability of evapotranspiration - The role of surface type and vegetation.
738 Ph.D. Thesis, University Of Copenhagen, Department Of Geography and Geology, Denmark.
- 739 • Rosero, E., Yang, Z.-L., Wagener, T., Gulden, L.E., Yatheendradas, S., Niu, G.-Y., 2010. Quantifying
740 parameter sensitivity, interaction, and transferability in hydrologically enhanced versions of the Noah
741 land surface model over transition zones during the warm season. *J. Geophys. Res.* 115, D03106.
742 doi:10.1029/2009JD012035
- 743 • Sahoo, G.B., Ray, C., De Carlo, E.H., 2006. Calibration and validation of a physically distributed
744 hydrological model, MIKE SHE, to predict streamflow at high frequency in a flashy mountainous
745 Hawaii stream. *J. Hydrol.* 327, 94–109. doi:10.1016/j.jhydrol.2005.11.012
- 746 • Schelde, K., Ringgaard, R., Herbst, M., Thomsen, A., Friborg, T. and Søgaard, H., 2011. Comparing
747 Evapotranspiration rates estimated from Atmospheric Flux and TDR Soil Moisture Measurements,
748 *Vadose Zone J.*, 10, 78–83, doi:10.2136/vzj2010.0060.
- 749 • Schulze, E.-D., Kelliher, F.M., Korner, C., Lloyd, J., Leuning, R., 1994. Relationships among maximum
750 stomatal conductance, ecosystem surface conductance, carbon assimilation rate, and plant nitrogen
751 nutrition: a global ecology scaling exercise. *Annu. Rev. Ecol. Syst.* 629–660. doi:
752 10.1146/annurev.es.25.110194.003213.

- 753 • Shrestha, P., Sulis, M., Masbou, M., Kollet, S., Simmer, C., 2014. A Scale-Consistent Terrestrial Systems
 754 Modeling Platform Based on COSMO, CLM, and ParFlow. *Mon. Weather Rev.* 142, 3466–3483.
 755 doi:10.1175/MWR-D-14-00029.1
- 756 • Shuttleworth, W.J., Wallace, J.S., 1985. Evaporation from sparse crops-an energy combination theory.
 757 *Q.J.R. Meteorol. Soc.* 111, 839–855. doi:10.1002/qj.49711146910
- 758 • Sonnenborg, T. O., Pang, B., Brøge, A., Christiansen, J. R., Stisen, S., Gundersen, P., 2013. Modeling of
 759 evapotranspiration and groundwater recharge from forest. TR32-HOBE symposium, Bonn, Germany.
- 760 • Stisen, S., McCabe, M.F., Refsgaard, J.C., Lerer, S., Butts, M.B., 2011a. Model parameter analysis using
 761 remotely sensed pattern information in a multi-constraint framework. *J. Hydrol.* 409, 337–349.
 762 doi:10.1016/j.jhydrol.2011.08.030
- 763 • Stisen, S., Sonnenborg, T.O., Højberg, A.L., Trolborg, L., Refsgaard, J.C., 2011b. Evaluation of Climate
 764 Input Biases and Water Balance Issues Using a Coupled Surface–Subsurface Model. *Vadose Zone J.* 10,
 765 37. doi:10.2136/vzj2010.0001
- 766 • Stisen, S., Højberg, A. L., Trolborg, L., Refsgaard, J. C., Christensen, B. B. S., Olsen, M., Henriksen, H.
 767 J., 2012. On the importance of appropriate precipitation gauge catch correction for hydrological
 768 modelling at mid to high latitudes. *Hydrol. Earth Syst. Sc.*, 16, 4157–4176, doi:10.5194/hess-16-4157-
 769 2012.
- 770 • Stoy, P. C., Mauder, M., Foken, T., Marcolla, B., Boegh, E., Ibrom, A., Arain, M.A., Arneth, A., Aurela,
 771 M., Bernhofer, C., others, 2013. A data-driven analysis of energy balance closure across FLUXNET
 772 research sites: The role of landscape scale heterogeneity. *Agric. For. Meteorol.* 171, 137–152.
- 773 • Styczen, M., Hansen, S., Jensen, L. S., Svendsen, H., Abrahamsen, P., Børgesen, C. D., Thirup, C.,
 774 Østergaard, H. S., 2004a. Standardopstillinger til Daisy-modellen. Vejledning og baggrund. Version 1.2,
 775 april 2006. DHI Institut for Vand og Miljø, Denmark.
- 776 • Styczen, M., Hansen, S., Jensen, L. S., Svendsen, H., Abrahamsen, P., Børgesen, C. D., Thirup, C.,
 777 Østergaard, H. S., 2004b. Appendix-samling, DHI Institut for Vand og Miljø, Denmark.

- 778 • Sun, G., Noormets, A., Chen, J., McNulty, S. G., 2008. Evapotranspiration estimates from eddy
779 covariance towers and hydrologic modeling in managed forests in Northern Wisconsin, USA, *Agr.*
780 *Forest. Meteorol.*, 148, 257–267, doi:10.1016/j.agrformet.2007.08.010.
- 781 • Sun, Y., Hou, Z., Huang, M., Tian, F., Ruby Leung, L., 2013. Inverse modeling of hydrologic parameters
782 using surface flux and runoff observations in the Community Land Model. *Hydrol. Earth. Syst. Sc.* 17,
783 4995–5011. doi:10.5194/hess-17-4995-2013
- 784 • Thompson, J.R., Sørensen, H.R., Gavin, H., Refsgaard, A., 2004. Application of the coupled MIKE
785 SHE/MIKE 11 modelling system to a lowland wet grassland in southeast England. *J. Hydrol.* 293, 151–
786 179. doi:10.1016/j.jhydrol.2004.01.017
- 787 • Topping, C., Olsen, J., 2006. Vegetation growth simulation in ALMaSS. Danish Ministry of the
788 Environment report: Ukrudtsstriglingens effekter på dyr planter og ressourceforbrug, Appendix B,
789 Danish Ministry of the Environment, Copenhagen, Denmark.
- 790 • Twine, T.E., Kustas, W.P., Norman, J.M., Cook, D.R., Houser, Pr., Meyers, T.P., Prueger, J.H., Starks,
791 P.J., Wesely, M.L., 2000. Correcting eddy-covariance flux underestimates over a grassland. *Agric. For.*
792 *Meteorol.* 103, 279–300.
- 793 • van Genuchten, M. Th., 1980. A closed-form equation for predicting the hydraulic conductivity of
794 unsaturated soils, *Soil Sci. Soc. Am. J.*, 44, 892–898. doi:10.2136/sssaj1980.03615995004400050002x.
- 795 • Van der Keur, P., Hansen, S., Schelde, K., Thomsen, A., 2001. Modification of DAISY SVAT model for
796 potential use of remotely sensed data. *Agric. For. Meteorol.* 106, 215–231.
- 797 • Wang, Q., Tenhunen, J., Falge, E., Bernhofer, C.H., Granier, A., Vesala, T., 2004. Simulation and scaling
798 of temporal variation in gross primary production for coniferous and deciduous temperate forests. *Glob.*
799 *Change Biol.* 10, 37–51. doi:10.1046/j.1529-8817.2003.00716.x.
- 800 • Wilson, K., Goldstein, A., Falge, E., Aubinet, M., Baldocchi, D., Berbigier, P., Bernhofer, C., Ceulemans,
801 R., Dolman, H., Field, C., others, 2002. Energy balance closure at FLUXNET sites. *Agric. For. Meteorol.*
802 113, 223–243.

- 803 • Wösten, J. H. M., Lilly, A., Nemes, A., Le Bas, C., 1999. Development and use of a database of
804 hydraulic properties of European soils, *Geoderma*, 90,169–185, doi:10.1016/S0016-7061(98)00132-3.
- 805 • Xevi, E., Christiaens, K., Espino, A., Sewnandan, W., Mallants, D., Sørensen, H., Feyen, J., 1997.
806 Calibration, validation and sensitivity analysis of the MIKE-SHE model using the Neuenkirchen
807 catchment as case study. *Water Resour. Manag.*11, 219–242.
- 808 • Zhou, M.C., Ishidaira, H., Hapuarachchi, H.P., Magome, J., Kiem, A.S., Takeuchi, K., 2006. Estimating
809 potential evapotranspiration using Shuttleworth–Wallace model and NOAA-AVHRR NDVI data to feed
810 a distributed hydrological model over the Mekong River basin. *J. Hydrol.* 327, 151–173.
811 doi:10.1016/j.jhydrol.2005.11.013
- 812 • Zweifel, R., Böhm, J.P., Häsler, R., 2002. Midday stomatal closure in Norway spruce—reactions in the
813 upper and lower crown. *Tree Physiol* 22, 1125–1136.

814

Fig1

[Click here to download high resolution image](#)

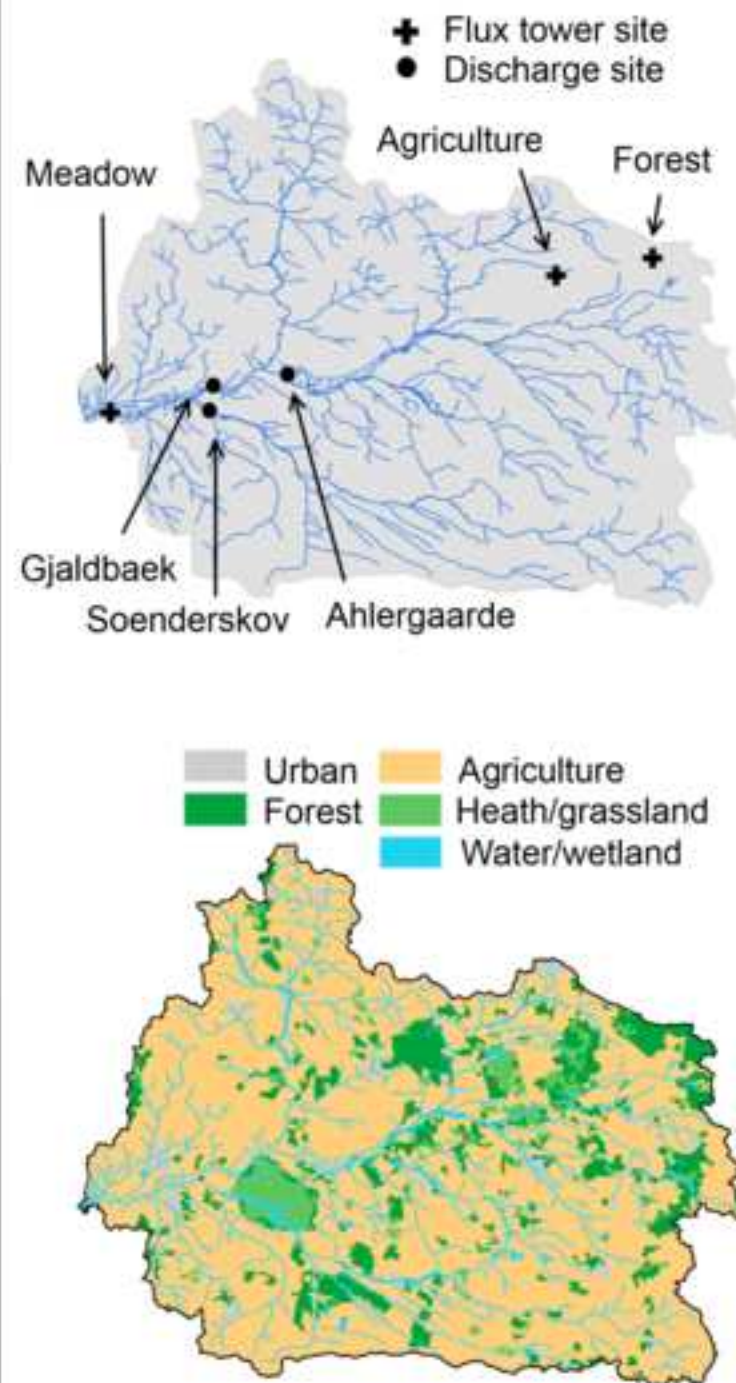
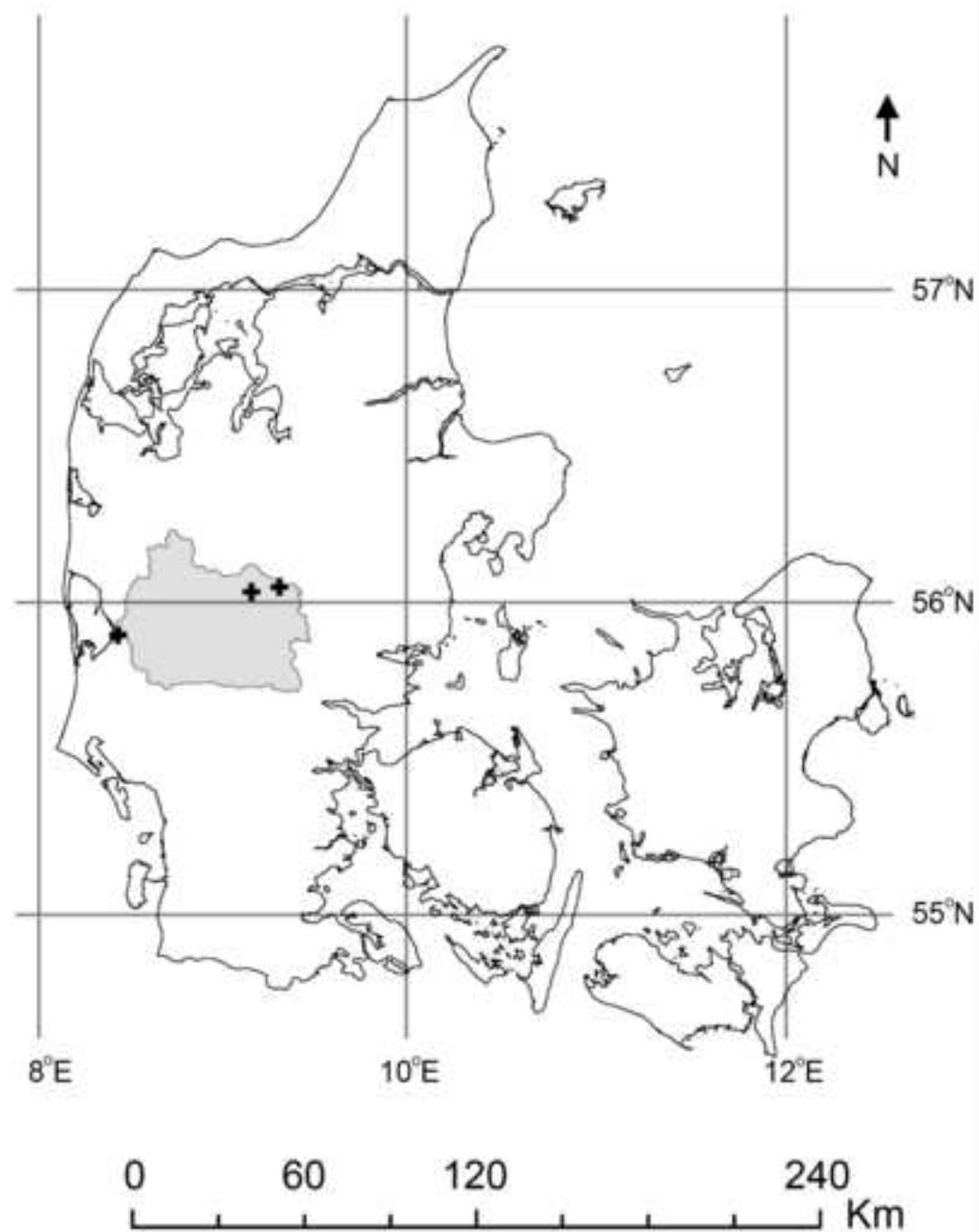


Fig2

[Click here to download high resolution image](#)

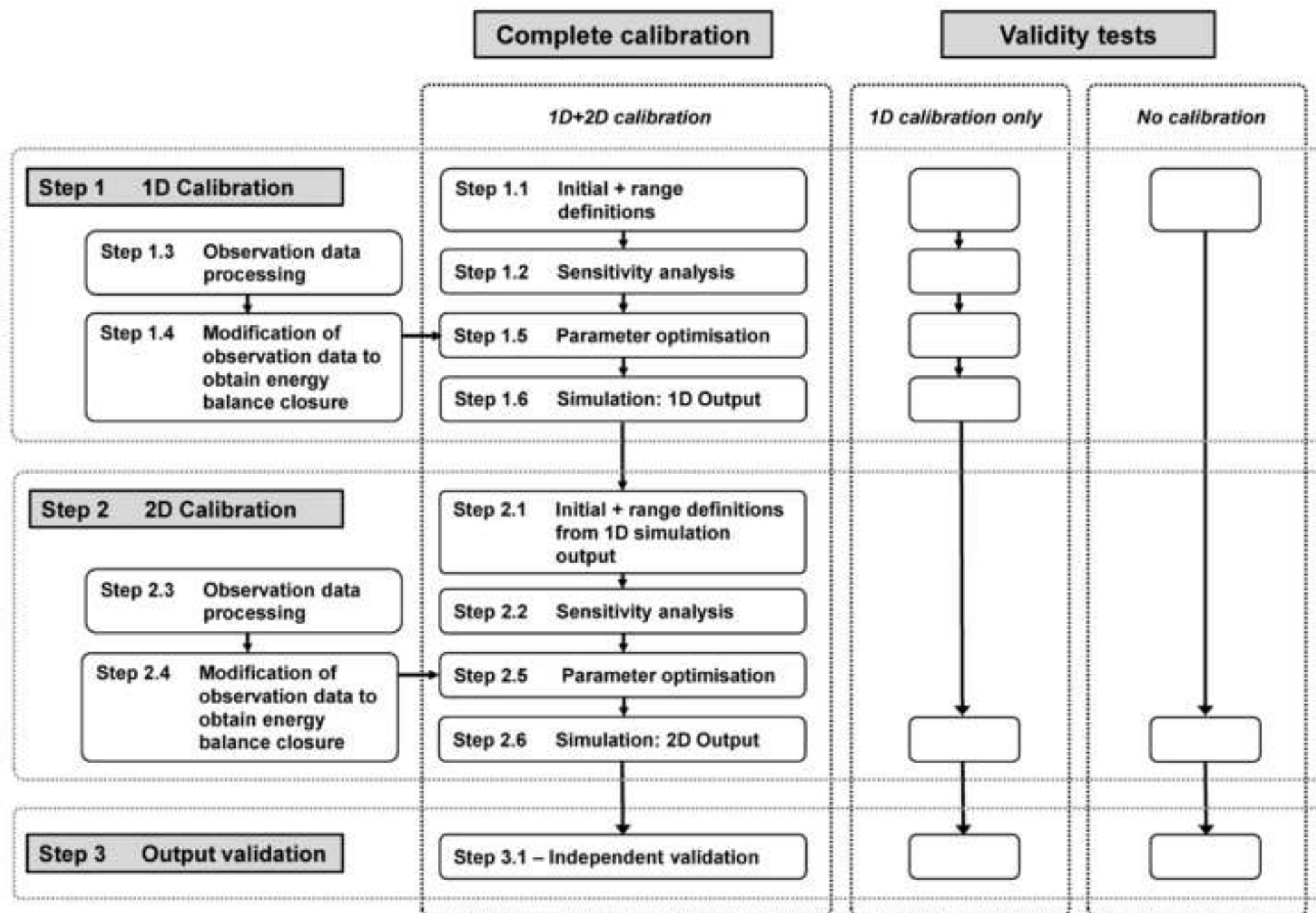


Fig3

[Click here to download high resolution image](#)

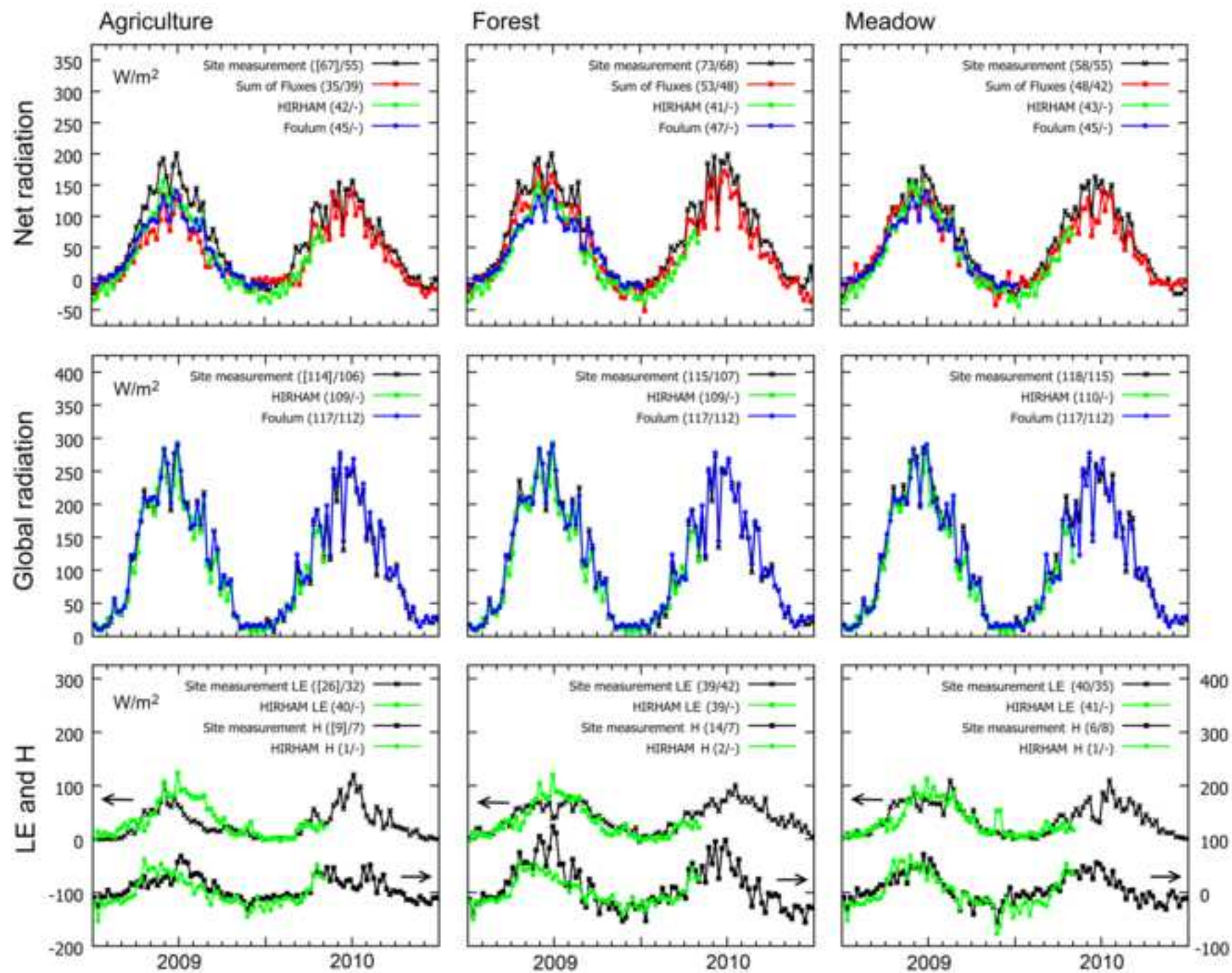


Fig4
[Click here to download high resolution image](#)

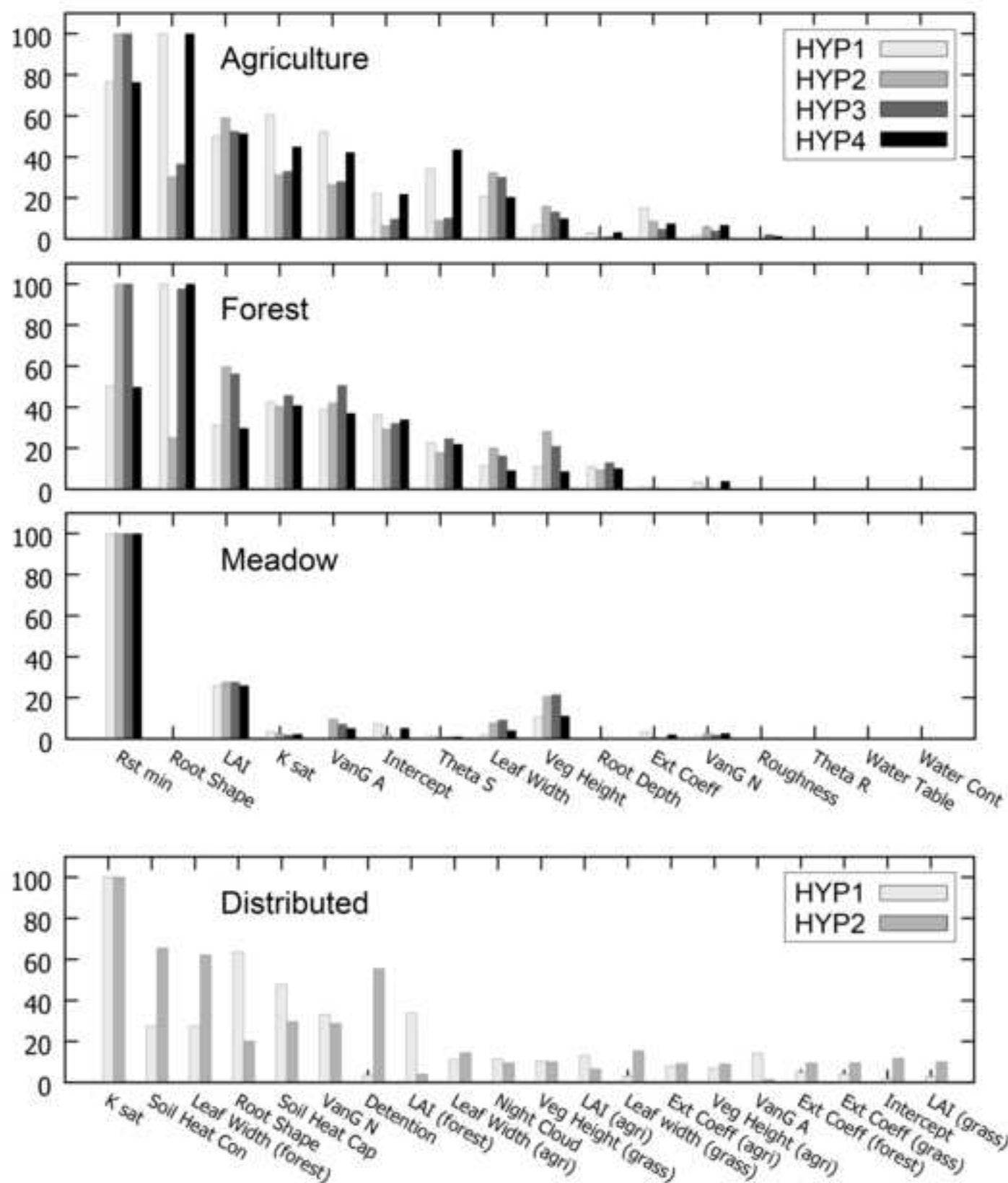


Fig5

[Click here to download high resolution image](#)

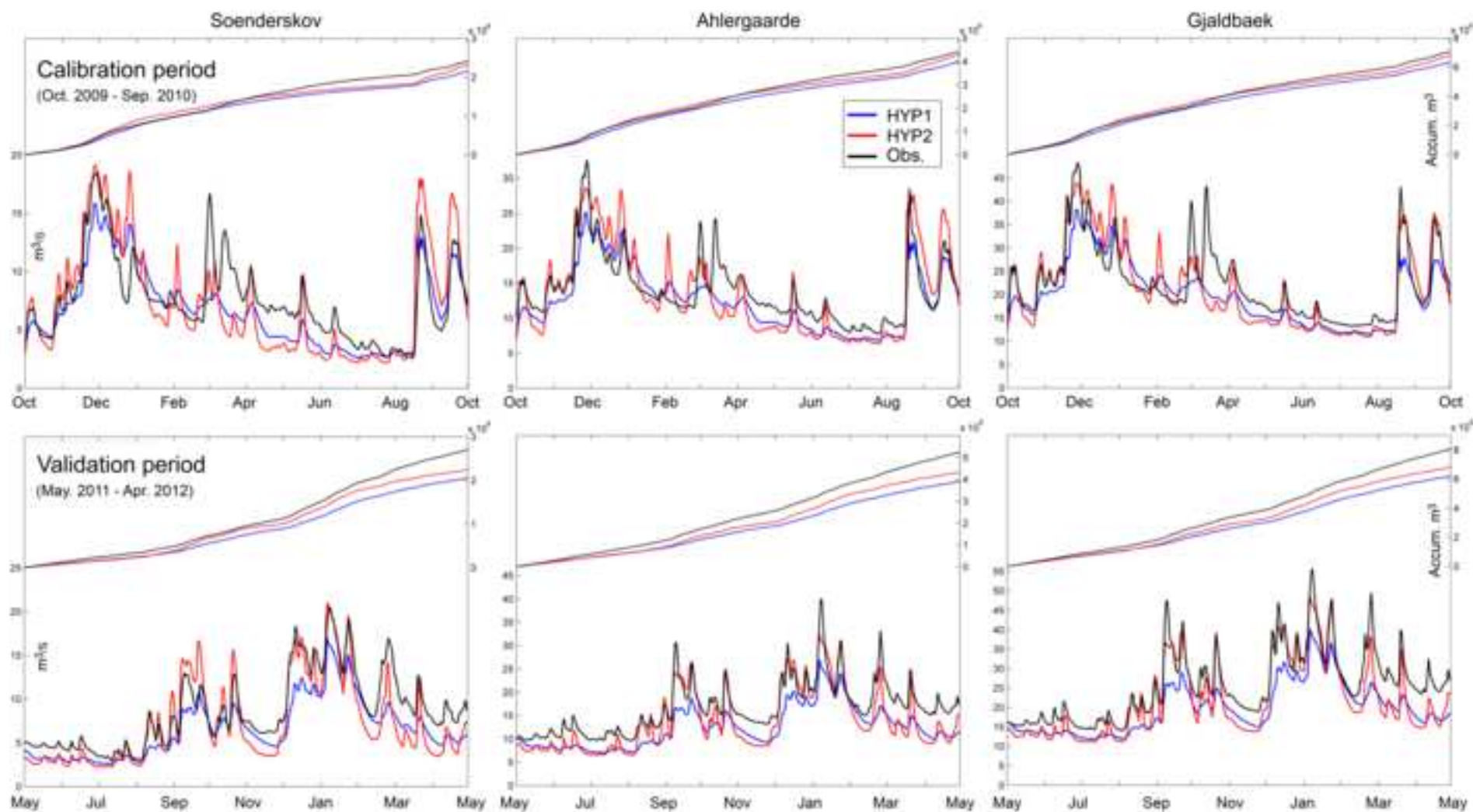


Fig6
[Click here to download high resolution image](#)

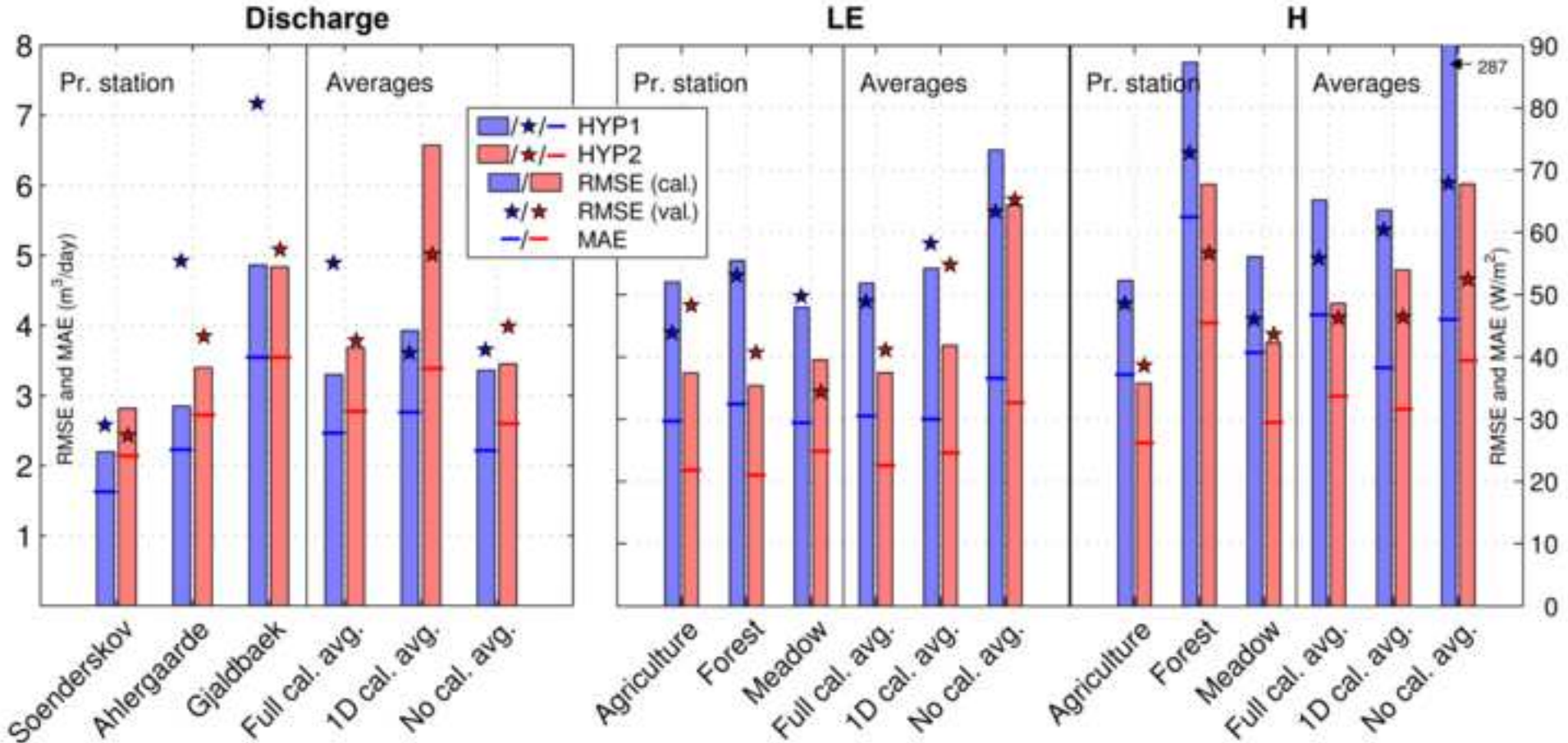


Fig7

[Click here to download high resolution image](#)

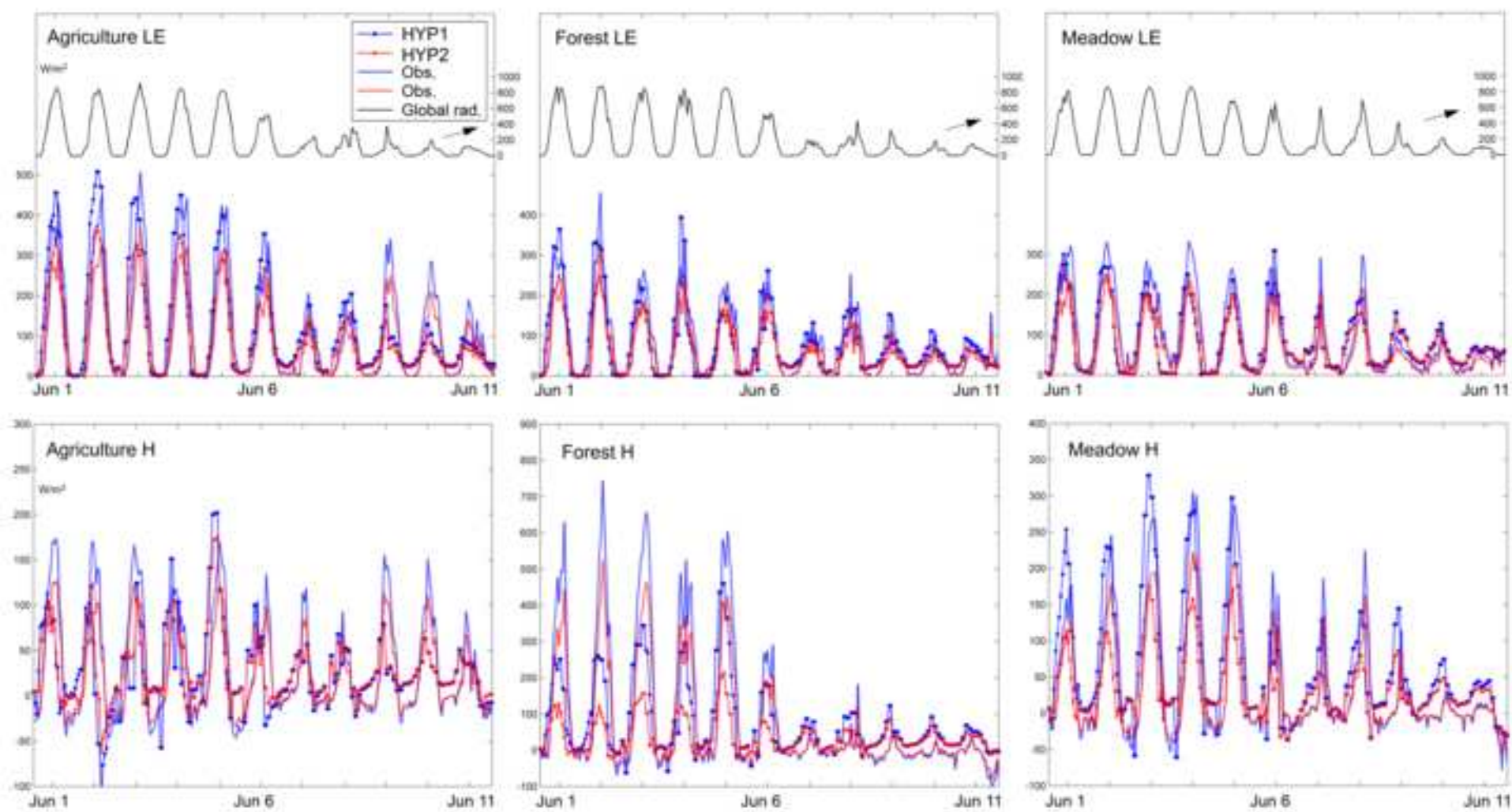


Fig8

[Click here to download high resolution image](#)

